



Examining the past 120 years' climate dynamics of Ethiopia

Mulatu Liyew Berihun^{1,2,3} · Atsushi Tsunekawa² · Nigussie Haregeweyn⁴ · Mitsuru Tsubo² · Hiroshi Yasuda⁵ · Ayele Almaw Fenta² · Yihun Taddele Dile⁶ · Haimanote Kebede Bayabil¹ · Seifu Admassu Tilahun^{3,7}

Received: 31 March 2023 / Accepted: 21 July 2023 / Published online: 16 August 2023
© The Author(s) 2023

Abstract

Climate change is one of the environmental threats around the globe. However, this change is not uniform throughout the world, both spatially and temporally. This study, therefore, examined the spatiotemporal (annual and seasonal) variability and trends of rainfall and temperature over Ethiopia from 1901 to 2020. Monthly rainfall and temperature (maximum, minimum, and mean) data were extracted from the latest version of the Climatic Research Unit (CRU 4.05) dataset. Using long-term seasonal rainfall patterns and pixel-based correlation techniques, five homogeneous rainfall zones were identified. The rainfall and temperature from CRU were validated using observed data from 235 and 145 meteorological stations, respectively. The results revealed that inter-seasonal rainfall and temperature variabilities are more pronounced than interannual variabilities in all rainfall zones. Only 19% (215,700 km²) and 3% (33,900 km²) of the country's total area experienced statistically significant ($\alpha = 0.05$) decreasing and increasing trends of rainfall, respectively from 1901 to 2020. A statistically significant decreasing trend in rainfall with time was observed during the summer in only one zone that received rainfall in all months. A precipitation concentration index analysis revealed that the country exhibited a moderate to strongly irregular annual and seasonal rainfall distribution, except during the summer when the rainfall distribution was uniform. There was hence a high degree of rainfall seasonality throughout the study period. In addition to the devastating 1984 nationwide drought, Ethiopia also experienced local droughts for a number of 10 to 20 years. Unlike rainfall, there was a significant ($\alpha = 0.05$) spatiotemporal increasing trend of temperature over the country. The spatial and temporal increasing trend of mean temperature over 120 years ranged from 0.24°C to 1.92°C and 0.72°C to 1.08°C, respectively. This increasing trend was higher in two zones located in the western and northwest parts of Ethiopia and the inflection points occurred after the 1970s in all zones. It is noteworthy that the maximum temperature increased at a lower rate than the minimum temperature. The warming trends and changes in rainfall patterns are likely to increase the frequency of climate extreme events and impact ecosystem services. This study suggests that climate change-sensitive zones require more attention and further study to enhance awareness of climate change in Ethiopia and facilitate adaptation to climate change and inform actions to mitigate adverse effects.

Keywords Drought-prone · CRU · Climate change · Climate variability · Rainfall seasonality · East Africa

✉ Mulatu Liyew Berihun
mulatulyew@yahoo.com; mberihun@ufl.edu

¹ Department of Agricultural and Biological Engineering, Tropical Research and Education Center, Institute of Food and Agricultural Sciences, University of Florida, Homestead, FL 33031, USA

² Arid Land Research Center, Tottori University, 1390 Hamasaka, Tottori 680-0001, Japan

³ Faculty of Civil and Water Resources Engineering, Bahir Dar Institute of Technology, Bahir Dar University, P.O. Box 26, Bahir Dar, Ethiopia

⁴ International Platform for Dryland Research and Education, Tottori University, 1390 Hamasaka, Tottori 680-0001, Japan

⁵ Organization for Educational Support and International Affairs, Tottori University, Koyama Minami 4-101, Tottori 680-8550, Japan

⁶ NextEra Energy, Okeechobee Blvd Unit 1205, West Palm Beach, Florida, FL 33411, USA

⁷ Department of Ecosystem service and management, Texas A&M University, College Station, Texas, USA

1 Introduction

Climate change in the context of global warming is a serious threat to the global environment in the 21st century (IPCC 2019, 2014). The global temperature in 2019 had increased by $1.1 \pm 0.1^\circ\text{C}$ since the pre-industrial period (1850–1900), and by $0.20 \pm 0.08^\circ\text{C}$ compared to the temperature during 2011–2015, which is the warmest five-year period on record (World Meteorological Organization (WMO) 2019). This increase in global temperature has been associated with stronger warming of the daily minimum temperature (T_{\min}) than the maximum temperature (T_{\max}) (Easterling et al. 1997). Continental average temperatures typically show greater variability than the global mean (IPCC 2014; WMO 2020). The continent of Africa is one of the most susceptible regions in the world to climate change. The historical climate record for Africa shows warming during the 20th century by approximately 0.7°C that has resulted in a decrease of precipitation over large portions of the continent (Desanker 2002). Predictions of climate under different emission scenarios have also indicated future warming over the continent ranging from 0.2°C to above 0.5°C per decade (Woodfine 2009). These warming trends and changes in precipitation patterns are likely to increase the occurrence of climate extremes such as droughts, floods, and storms as well as impact environmental ecosystem services (e.g., Berihun et al. 2020; Berihun et al. 2019; Fenta et al. 2017; Stojanovic et al. 2022; Woodfine 2009; van der Esch et al. 2017). Climate change has had a greater impact and extreme events have been more frequent in Sub-Saharan Africa (e.g., Dai et al. 1998; Degefu et al. 2017; Serdeczny et al. 2017). Unlike temperature, the amounts of precipitation in most parts of this region are likely to decrease, whereas rainfall is expected to become more variable (IPCC 2014; Gebrechorkos et al. 2019; Serdeczny et al. 2017; Wainwright et al. 2019; WMO 2020).

Climate change has been observed since the 1940s in Ethiopia, where rain-fed agricultural activity serves as the backbone of the economy but is disrupted by frequent droughts (e.g., Cheung et al. 2008; Easterling et al. 2000; Seleshi and Zanke 2004; Simane et al. 2016; Stojanovic et al. 2022; Wagesho et al. 2013). However, the apparent change of the climate varies as a function of the spatiotemporal scale of the analysis and the length of the study period (e.g., Cheung et al. 2008; Seleshi and Zanke 2004). The average temperature has increased by approximately $0.2\text{--}0.5^\circ\text{C}$ per decade, whereas average annual rainfall over the country has remained stable over the last 50 years (e.g., Cheung et al. 2008; Jury and Funk 2013). Previous studies in different local parts of Ethiopia have reported results comparable to those from national studies on spatiotemporal variability and trends in past climates (e.g., Alemayehu

et al. 2020; Alemu and Bawoke 2020; Asfaw et al. 2018; Bekuma et al. 2022; Belay et al. 2021; Conway et al. 2004; Habte et al. 2021; Mengistu et al. 2014; Mewded et al. 2022; Mulugeta et al. 2019; Tekleab et al. 2013). However, under local conditions, the spatiotemporal variabilities of rainfall and temperature are high and do not reflect large-scale climate trends (e.g., Asfaw et al. 2018; Conway et al. 2004; Mengistu et al. 2014; Mewded et al. 2022).

Climate change poses a significant threat to Ethiopia because the country lacks the adaptive capacity and resilience of socio-economic systems (Serdeczny et al. 2017). The irregular spatiotemporal distribution, variations, and temporal trends of climate have affected the food security of the country (Conway and Schipper 2011; Simane et al. 2016). Smallholder farmers are mostly affected by this problem because of their reliance on agricultural activities (e.g., Abeje et al. 2019). Long-term spatiotemporal analysis of climate (in terms of distribution, variability, and trend) is thus profoundly important for planning adaptive and mitigative measures for the challenges posed by climate change. Many previous studies have tried to elucidate the spatiotemporal distribution, variability, and trends of Ethiopia's past climate at regional (e.g., Bayable et al. 2021; Habte et al. 2021), basin (e.g., Cheung et al. 2008; Gurara et al. 2022; Mengistu et al. 2014; Mewded et al. 2022; Mulugeta et al. 2019), and watershed scales (e.g., Alemayehu et al. 2020; Asfaw et al. 2018; Berihun et al. 2019). However, there has been only limited research conducted on a national scale insofar as we know. Because the record of rainfall and temperature in Ethiopia covers less than 50 years in most parts of the country and includes missed and limited observations of rainfall and temperature. Given these limitations, previous national-scale studies have relied on observed rainfall and temperature datasets for climate analysis (e.g., Abebe et al. 2022; Jury and Funk 2013; Korecha and Barnston 2007; Seleshi and Zanke 2004). To overcome the spatiotemporal limitations of the observed data, recent studies of climate in Ethiopia (mainly watershed to regional-scale studies) have used different high-resolution satellite and reanalysis rainfall and temperature datasets such as the Tropical Rainfall Measuring Mission (TRMM), Climate Hazards Group InfraRed Precipitation with Station data (CHIRPS), Global Precipitation Climatology Centre (GPCC), and Climatic Research Unit (CRU) for spatiotemporal climate analyses (e.g., Alemu and Bawoke 2020; Asfaw et al. 2018; Degefu et al. 2017; Fenta et al. 2017; Mulugeta et al. 2019). Unlike the other datasets, the CRU dataset (<https://crudata.uea.ac.uk/cru/data/hrg/>) is the only reanalysis dataset that comprises gridded ($0.5^\circ \times 0.5^\circ$) resolution monthly rainfall and temperature (minimum, maximum, and mean) data for more than a century (since 1901, Harris et al. 2020). Previous studies have also used the CRU dataset for different climate applications and long-term spatiotemporal climate analysis in Ethiopia (e.g., Asfaw et al. 2018; Degefu et al. 2017; Dinku et al. 2008; Gurara et al.

2022; Tsidu 2012) and elsewhere (e.g., Ahmed et al. 2019; Ayugi et al. 2016; Broman et al. 2020). However, most of the studies conducted in Ethiopia have been limited to local or basin-scale analysis and have been inconsistent in their reporting of the results of climate change. National studies of the variability and distribution of rainfall and temperature at annual and seasonal timescales would greatly facilitate devising effective adaptation and mitigation plans for the country. Furthermore, it is necessary to predict climate extremes (e.g., flood and drought) accurately and to take appropriate adaptation and mitigation measures (e.g., Alhamsry et al. 2019; Broman et al. 2020; Seleshi and Camberlin 2006).

To the best of our knowledge, there has been no rigorous statistical study of the spatiotemporal variability and trends of rainfall and temperature that covers all of Ethiopia and could reveal the temporal evolution of rainfall and temperature over a timeframe longer than a century. The goal of this study was, therefore, to explore the spatiotemporal variability, distribution, and trends of rainfall and temperature (minimum, maximum, and mean) in Ethiopia from 1901 to 2020 by validating the CRU dataset using observed rainfall and temperature data collected from 235 and 145 meteorological stations, respectively. The specific objectives were to examine (i) the spatiotemporal variation and distribution of seasonal and annual rainfall and temperature patterns; (ii) rainfall and temperature trends from 1901 to 2020; and (iii) the distribution of seasonal and annual rainfall indices (indices of precipitation concentration and rainfall anomalies).

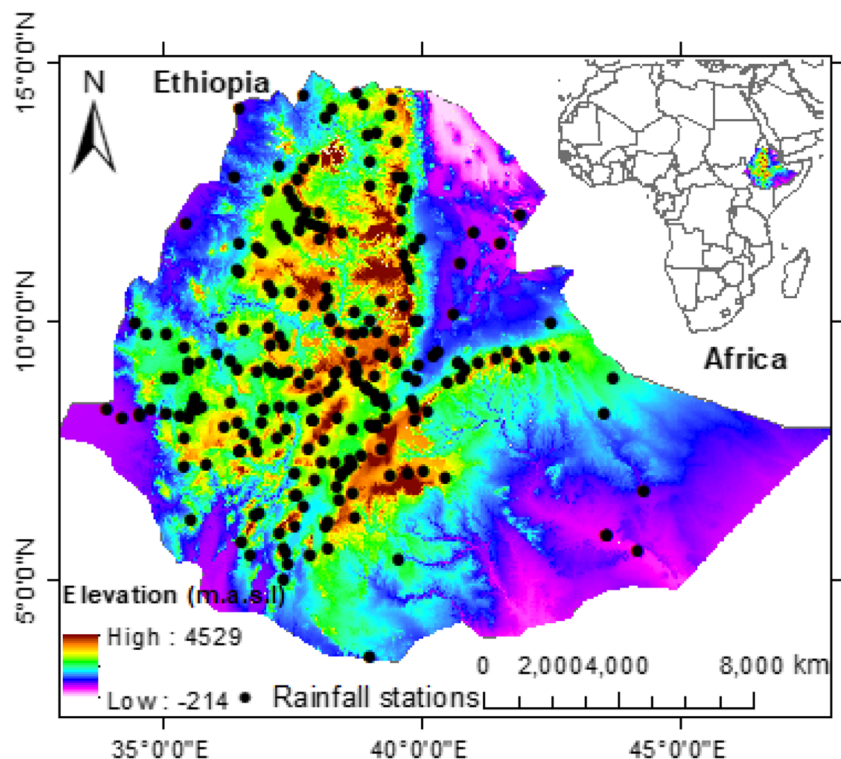
Unlike previous national-scale studies (Conway and Schipper 2011; Jury and Funk 2013; Korecha and Barnston 2007; Seleshi and Zanke 2004), this study identified five homogeneous rainfall zones using long-term (120 years) monthly and seasonal (winter, spring, summer, and autumn) rainfall patterns and magnitudes extracted from the CRU dataset at 365 grid points. Most previous national-scale studies have focused on specific parts of the country (mainly where rainfed agriculture is practiced), have been based on data from only a few meteorological stations, and have focused on the summer season (e.g., Diro et al. 2011; Korecha and Barnston 2007; Seleshi and Zanke 2004). This study relied on robust statistical software such as XLSTAT, R, and Python integrated with ArcGIS for the data analyses. We expect that the results will contribute to a better understanding of the past climate of Ethiopia in different rainfall zones and will inform future climate projections as well as adaptation and mitigation measures to be taken in response to the changing climate and extremes.

2 Research methods

2.1 Study area

The study area (Ethiopia) is in East Africa (Fig. 1) (33–48°E, 3–15°N) and covers an area of $\sim 1.13 \times 10^6$ km². Based on Digital Elevation Model (DEM) obtained from a 30 m Shuttle

Fig. 1 Locations and elevation map of meteorological stations in Ethiopia



Radar Topography Mission (SRTM), the topography is highly variable and consists of a complex of lowlands and highlands with elevations ranging from 214 m below sea level in the lowlands to 4529 m above sea level in the highlands. Ethiopia is in the tropical climate zone and lies between the Equator and the Tropic of Cancer. The country includes six main agro-ecological zones distinguished by their elevations and rainfall (Fenta et al. 2021; Hurni 1988). Ethiopia is characterized by large spatiotemporal variations in rainfall and temperature (Fazzini et al. 2015). The mean annual rainfall ranges from less than 200 mm to more than 1600 mm in the lowlands and highlands, respectively and the temperature is ranging from 50 °C in the lowland to 15 °C in the highlands (Fazzini et al. 2015).

Ethiopia has four rainfall seasons: *Bega* (winter; December, January, and February [DJF]), *Belg* (spring; March, April, and May [MAM]), *Kiremt* (summer; June, July, and August [JJA]) and *Tseday* (autumn; September, October, and November [SON]). In most parts of Ethiopia, *Bega* (winter) is the dry season. There is a small amount of rainfall in spring, but summer is the main rainy season. The seasonality of the rainfall is characterized by monomodal and bimodal rainfall patterns. These rainfall patterns are the most important determinants of the classification of the homogeneous rainfall zones in Ethiopia.

Ethiopia has the second-largest population in Africa after Nigeria (United Nations 2019), and approximately 80% of the population of Ethiopia lives in rural areas and depends mainly on agricultural activities for sustenance (CSA 2018).

2.2 Data used in the study

Both gridded and observed rainfall and temperature (minimum, maximum, and mean) datasets were used in this study. Gridded monthly rainfall and temperature (minimum, maximum, and mean) data were obtained from the current version of the CRU TSv4 dataset with $0.5^\circ \times 0.5^\circ$ resolution from 1901 to 2020 (120 years; Harris et al. 2020). We selected this dataset because of its fine spatial resolution and 120-year record length. The dataset was developed from available meteorological station data. The availability of data from these stations varied from 40% (at the start of the 20th century) to 70% (middle and second half of the 20th century) of the CRU grid cells (Harris et al. 2020). In this study, we used 365 grid points (one point from each grid was created by the fishnet tool in Arc-GIS environments) to extract the rainfall and temperature from the CRU dataset (Fig. 2). Observed daily rainfall and temperature data from 1981 to 2014 were obtained from 235 and 145 meteorological stations, respectively, of the National Meteorology Agency of Ethiopia (<http://www.ethiomet.gov.et>). Prior to utilizing the observed rainfall and temperature data, it is crucial to conduct an analysis of its quality, which serves as a fundamental step. We used gridded daily rainfall (grid resolution of $0.05^\circ \times 0.05^\circ$) from the CHIRPS dataset

(Funk et al. 2015) from 1981 to 2014 to fill in missing values of observed rainfall. The CRU and CHIRPS datasets have been used in a manner similar to the way they were used in this study for climate analyses in Ethiopia and East Africa (e.g., Asfaw et al. 2018; Degefu et al. 2017; Fenta et al. 2017; Dinku et al. 2008; Mulugeta et al. 2019; Tsidu 2012; Wagesho et al. 2013). Unlike rainfall data, the missing observed monthly temperature data were compiled using the arithmetic mean method (Subramanya 2008). Moreover, the reliability of data recording was assessed to ensure a relatively consistent and homogeneous dataset. To achieve homogeneity, it is essential that the measurements were consistently collected using the same instrumentation, and method, in a consistent environment, and at the same time and location. Furthermore, outliers, which are data points that deviate significantly from the overall trend of the recorded data, were identified within the monthly rainfall series through a test for high and low outliers. Monthly rainfall and temperature data were aggregated using R software to create annual and seasonal time series for each rainfall zone (Section 2.3). The seasonal time-series data were aggregated based on the four climate seasons of Ethiopia.

2.3 Creating homogeneous rainfall zones

Categorizing the climate regions into different clusters based on their long-term characteristics can help to minimize potential uncertainties and facilitate the practical application of the results (Wagesho et al. 2013). Similarly, the design rainfall estimates of most hydraulic structures have also been based on three rainfall regions classified according to the unimodal and bimodal rainfall systems (ERA 2013). However, this classification technique cannot account for region/zone-specific rainfall patterns (e.g., Berhanu et al. 2014; Cheung et al. 2008; Seleshi and Zanke 2004). In this study, we, therefore, identified five homogenous rainfall zones (Fig. 2) based on the long-term pattern and magnitude of rainfall (monthly and seasonal), and we calculated spatial or pixel-based correlations using the following three steps: (1) we analyzed the monthly peaks (unimodal or bimodal), the amounts of seasonal rainfall, and patterns of long-term rainfall (hyetograph) for 365 grid points and five classes of rainfall (Fig. 2); (2) we calculated a pixel-based correlation coefficient (r) using long-term monthly rainfall to check the consistency of the pixels within each group. We fixed the threshold r value at 0.6 (satisfactory level), and (3) we moved pixels from one zone to a neighboring zone if the r -value of a given pixel was less than the threshold value. We carried out this procedure in steps until all the r values were equal to or greater than the fixed threshold value. Previous studies in Ethiopia have also tried to classify rainfall regions into different rainfall zones (e.g., Alhamsry et al. 2019; Degefu et al. 2017; Dinku et al. 2008; Tsidu 2012; Wagesho et al. 2013). However, these studies have not fully accounted for the amounts and patterns of

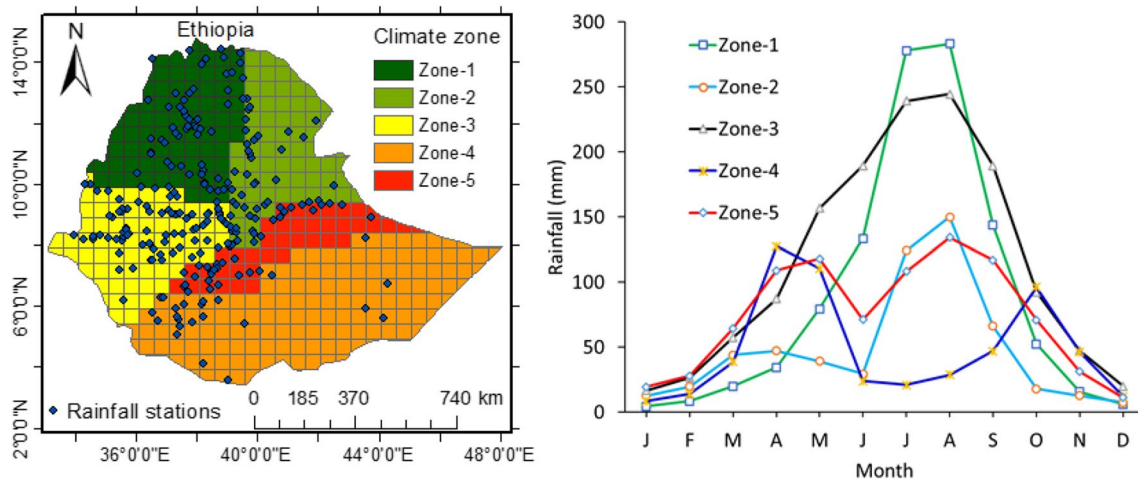


Fig. 2 Rainfall stations and five climate zones of Ethiopia (left) and monthly rainfall in each zone (right) analyzed on the basis of CRU long-term (1901–2020) monthly rainfall data

monthly and seasonal long-term rainfall, or they have lacked a spatial representation of classified zones.

2.4 Evaluation of CRU dataset

In this study, we compared the CRU dataset (rainfall and temperature) against rainfall and temperature (minimum and maximum) data recorded at weather stations in five rainfall zones on a yearly timescale for the period 1981–2014. Zonal average rainfall and temperature data were used to evaluate the applicability of the CRU dataset. For rainfall, data from 56, 44, 79, 23, and 33 stations were evaluated in Zone-1, Zone-2, Zone-3, Zone-4, and Zone-5, respectively. For temperature, data from 38, 21, 50, 13, and 23 stations in Zone-1, Zone-2, Zone-3, Zone-4, and Zone-5, respectively, were likewise used to evaluate the CRU temperature dataset. For this purpose, the monthly CRU dataset was extracted for each rainfall and temperature station. The average rainfall for each rainfall zone was estimated using an area-weighted approach. Commonly used statistical measures: the coefficient of determination (R^2) associated with the linear regression, the mean error (ME), the mean absolute error (MAE), the percent bias ($PBIAS$), and the Nash–Sutcliffe efficiency (NSE) were used to evaluate the accuracy of the gridded dataset at an annual timescale. This type of evaluation approach has been applied in previous climate studies (e.g., Ayugi et al. 2016; Cheung et al. 2008; Mewded et al. 2022).

2.5 Climate variability and trend detection

2.5.1 Coefficient of variation (CV)

The interannual and inter-seasonal variability of rainfall and temperature data (minimum, maximum, and mean) were

quantified by the coefficient of variation (CV) at spatial and temporal scales. The CV s were calculated using Eq. 1 at seasonal and annual scales.

$$CV = \frac{\sigma}{\mu} \times 100 \quad (1)$$

where σ is the standard deviation and μ is the mean of the rainfall or temperature data. Higher CV values indicate a higher degree of variability in rainfall and temperature, and vice versa.

2.5.2 Spatiotemporal rainfall and temperature trend detection

We used Mann–Kendall (MK; Burn 1994) and Pettitt (Pettitt 1979) tests to analyze the long-term trends in annual, seasonal, and monthly rainfall and temperature (minimum, maximum, and mean) time-series data. These methods have been widely applied in previous studies (e.g., Alemu and Bawoke 2020; Conway et al. 2004; Habte et al. 2021; Mengistu et al. 2014; Tekleab et al. 2013) to analyze monotonic (increasing or decreasing), homogeneous trends in various climate analyses. The statistical significance of trends was also evaluated using these methods.

We also used Sen's slope estimator to estimate the slope of the rainfall and temperature trends. In the case of a linear trend, Sen's slope estimator can also be used to estimate the magnitude of the monotonic trend as follow:

$$\beta = \text{median} \left(\frac{x_j - x_i}{j - i} \right) \quad (2)$$

where β represents the median value of the slopes between data measurements x_i and x_j at time steps i and j ($i < j$), respectively. Compared with linear regression, this method has the advantage of limiting the impact of outliers or missing values on the slope. The temporal and spatial analysis of MK trends were done by using XLSTAT software, R and Python packages integrated with ArcGIS 10.4 tool, respectively.

2.5.3 Precipitation concentration index (PCI)

PCI (Oliver 1980) was used to estimate the variability or distribution pattern of annual and seasonal rainfall in different rainfall zones. The PCI values were calculated using equations 3 and 4 at annual and seasonal timescales, respectively.

$$PCI = \frac{\sum_{i=1}^{12} P_i^2}{\left(\sum_{i=1}^{12} P_i\right)^2} \times 100 \quad (3)$$

$$SPCI = \frac{\sum_{i=1}^3 P_i^2}{\left(\sum_{i=1}^3 P_i\right)^2} \times 25 \quad (4)$$

where P is monthly rainfall during month i . The values of PCI and $SPCI$ were assigned to four classes as follows: 1) values below 10 indicates a uniform rainfall distribution; 2) values of 11–15 indicate a moderate amount of precipitation; 3) values of 16–20 indicate an irregular distribution; and 4) values above 20 indicate a highly irregular distribution of precipitation throughout the year. This method has been applied in previous local and regional studies in Ethiopia (e.g., Belay et al. 2021; Fenta et al. 2017).

2.5.4 Standardized precipitation anomaly index (SPI)

As in previous studies in different parts of Ethiopia (e.g., Alemayehu et al. 2020; Alemu and Bawoke 2020; Asfaw et al. 2018; Bayable et al. 2021; Belay et al. 2021; Fenta et al. 2017; Habte et al. 2021; Mengistu et al. 2014), we used equation 5 to calculate the spatial and temporal SPI to analyze the long-term dry and rainy years in the study area at seasonal and annual timescales. We also used the SPI to assess the magnitude of drought years.

$$SPI_i = \frac{X_i - \bar{X}}{\sigma} \quad (5)$$

where X_i stands for the annual rainfall in year i , and \bar{X} and σ are the long-term mean annual rainfall and standard deviation over the period of observation, respectively. The SPI values were assigned to one of seven classes based on

McKee et al. (1993): Extremely wet ($SPI > 2$), very wet ($1.5 > SPI < 2$), wet ($1.0 > SPI < 1.5$), normal ($-1 > SPI < 1$), dry ($-1 < SPI > -1.5$), very dry ($-1.5 < SPI > -2$), and extremely dry ($SPI < -2$). Negative SPI values indicate a drought (deficit years) period, and positive values indicate a wet (excess years) period. Long-term seasonal and annual temperature anomalies were also calculated for each rainfall zone in the study area.

3 Results and discussion

3.1 Validation of CRU dataset across five rainfall zones

Fig. 3 shows the results of comparing the extracted CRU rainfall and temperature data with gauge-based observation data across five rainfall zones. The results showed that the monthly CRU rainfall and temperature (Tmin and Tmax) data in all rainfall zones were strongly correlated with the observed data. The agreement between the CRU and observed rainfall data was better in Zone-1, Zone-2, and Zone-3 than in Zone-4 and Zone-5 (Fig. 3a). This agreement was evidenced across the rainfall zones by the value of R^2 , which ranged from 0.76 in Zone-4 to 0.95 in Zone-1, and the NSE , which ranged from 0.72 in Zone-4 to 0.93 in Zone-1. The higher values of R^2 and NSE were most likely related to the number of stations found in each rainfall zone. The greater the number of stations in a rainfall zone, the better the agreement between the CRU dataset and observed rainfall. Unlike the values of R^2 and NSE , the values of ME (0.35), MAE (0.35), and $PBIAS$ (0.44) were relatively better in Zone-4 than in the other zones (Fig. 3a). The evaluation results also showed that the monthly CRU temperatures (Tmin and Tmax) were closely correlated with the corresponding temperature data from stations (Fig. 3b and 3c). The fact that the correlation of the CRU data was higher with the observed Tmax than the observed Tmin was evidenced by all the statistical metrics of correlation in all rainfall zones (Fig. 3b and 3c). However, the degree of correlation with CRU data was lower for observed temperatures (Tmin and Tmax) than for rainfall (Fig. 3). The smaller number of temperature stations in comparison to rainfall stations may contribute to this phenomenon. Additionally, uncertainty in temperature measurement arises from the quality of data obtained during the measurement process. Unlike rainfall measurement, which can be relatively straightforward, temperature data is predominantly collected manually at most stations, making it a more challenging task, and producing errors. Moreover, managing the missing data for temperature and rainfall is different, which may affect the correlation values. Unlike other some studies conducted at the watershed

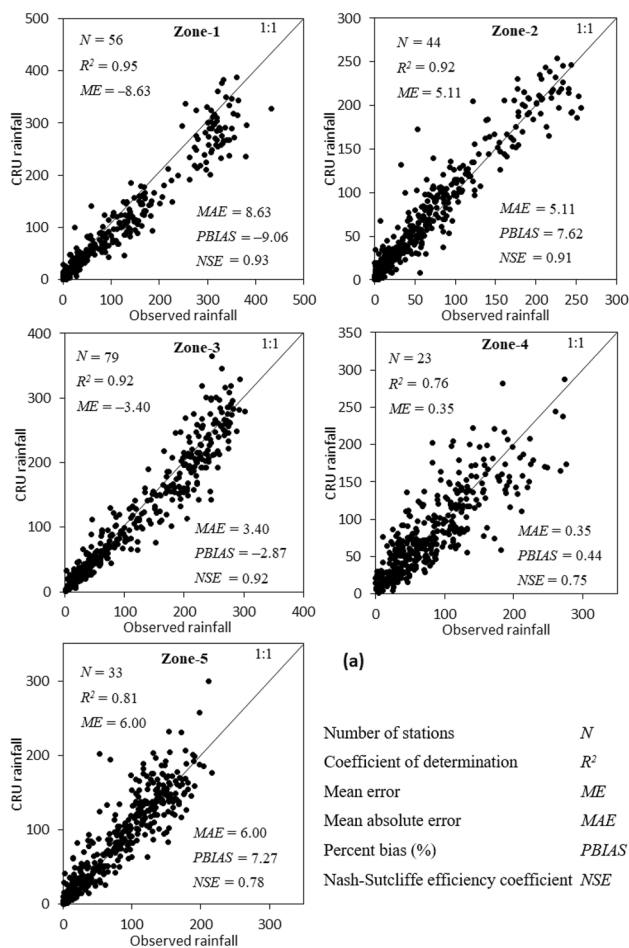


Fig. 3 Comparison of monthly CRU rainfall (mm) (a), minimum temperature (Tmin, °C) (b), and maximum temperature (Tmax, °C) (c) with gauge data for the five climate zones of Ethiopia during 1981–2014. *N* indicates the number of gauge stations in each zone that were considered for evaluation

and basin scale, the strong correlation between observed data and CRU datasets in our study can be attributed to the reduction of errors by averaging the data at the zonal level. It is important to note that the comparison was performed at the zonal level rather than at individual gauge stations.

A limited number of studies have evaluated gridded datasets in Ethiopia, and studies in some parts of Ethiopia have reported a strong correlation between CRU data and observed rainfall and temperature data (e.g., Degefu et al. 2017; Dinku et al. 2008; Gurara et al. 2022; Mulugeta et al. 2019; Tsidu 2012). However, a study in the Woleka subbasin (Zone-1) showed that the observed rainfall and temperature data were not significantly correlated with the CRU data (e.g., Asfaw et al. 2018). Studies similar to ours but carried out elsewhere (e.g., Ahmed et al. 2019; Ayugi et al. 2016; Broman et al. 2020; Ongoma and Chen 2017) have also evaluated the comparability of CRU datasets by comparing CRU data with gauged and other

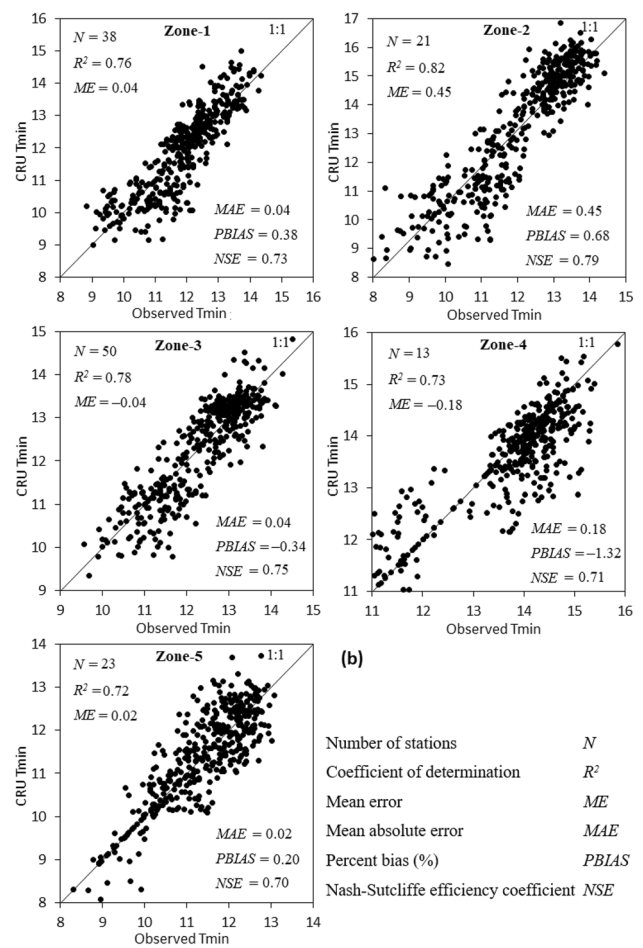


Fig. 3 (continued)

available gridded data (e.g., GPCP and CHRIPS) for variability and trend analysis. The weak correlations between observed and CRU datasets are most likely attributable to the number of gauges and quality of observed data (e.g., Asfaw et al. 2018; Dinku et al. 2008; Mulugeta et al. 2019). Because of the number of uncertainties, the risk of using the gridded dataset is much lower than the risk of using low-grade observed data (Wagesho et al. 2013).

3.2 Spatial and temporal variability and trend of rainfall

3.2.1 Inter-annual spatial and temporal variability and trend of rainfall

The fact that the mean annual rainfall in Ethiopia for the last 120 years was 890 mm ±106 mm indicates that there has been a high degree of spatial variability of rainfall in the country. The rainfall ranged from less than 200 mm ±80 mm (most of the lowland areas) to greater than 1500 mm ±125 mm (most of the highland areas) (Fig. 4). Zonal

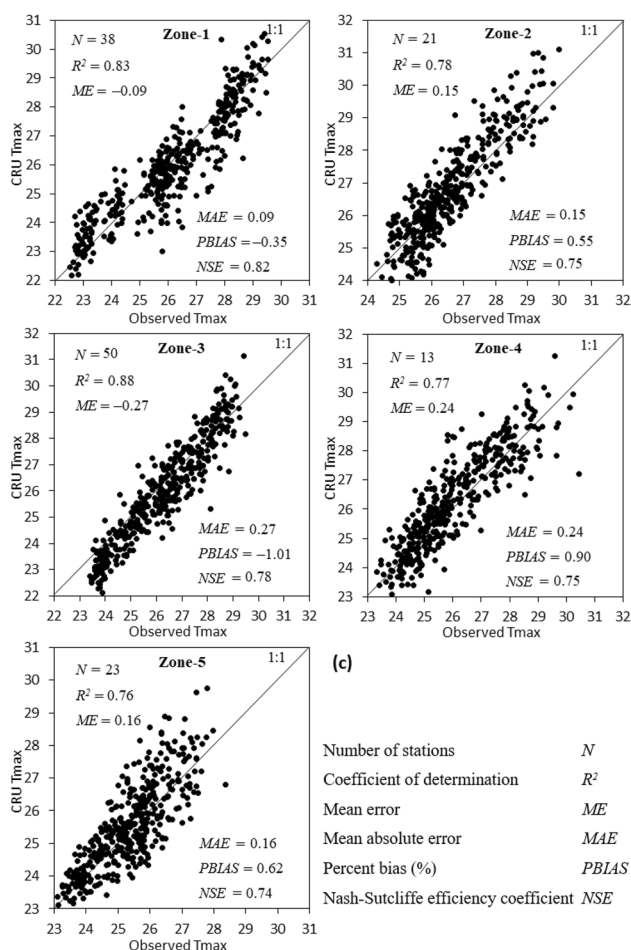


Fig. 3 (continued)

level analysis has shown that the mean annual rainfall (in increasing order) was 540 mm \pm 80 mm (Zone-4), 560 mm \pm 90 mm (Zone-2), 880 mm \pm 120 mm (Zone-5), 1060 mm \pm 110 mm (Zone-1), and 1510 mm \pm 125 mm (Zone-3). The panel in the first row and second column of Fig. 4 shows the *CV* of the rainfall. This *CV* is a metric of the interannual variability of the annual rainfall in each rainfall zone. Most parts of Ethiopia exhibit low interannual variability of rainfall (Fig. 4). Moderate interannual variability of annual rainfall (*CV* \sim 37%) was especially apparent in some parts of Zone-2, Zone-4, and Zone-5 (Fig. 4). In contrast, the interannual variations of annual rainfall in regions such as Zone-1, Zone-3, and most parts of Zone-2 and Zone-5, which receive a high amount of rainfall, were small (*CV* < 15%; Fig. 4) over the study period.

The changes in the annual rainfall in Zone-1, Zone-2, Zone-3, and Zone-5 have been dominated by variations in June-to-August (JJA) rainfall. Conversely, in Zone-4, the variations in March-to-May (MAM) rainfall determine the change in the annual rainfall series. Although there have been few studies of the variability of annual rainfall over

Ethiopia, the results of a previous study by Wagesho et al. (2013) on spatial variability of annual rainfall over Ethiopia agree well with the findings of this study. The variations of rainfall across the rainfall zones of Ethiopia are attributed mainly to topographic variations. In most of the Ethiopian highland regions, topography has a major influence on the spatial patterns of rainfall (e.g., Alhamsry et al. 2019; Fenta et al. 2017; Stojanovic et al. 2022; Wagesho et al. 2013). In other words, the variation in rainfall across rainfall zones is closely linked to the sources of moisture in the regions (Stojanovic et al. 2022). The source of the rainfall in the northeast, southwest, and west (Zone-2, Zone-3, and some parts of Zone-4 and Zone-5) is primarily terrestrial moisture (more than 50%), whereas oceanic sources account for rainfall in the southeast (parts of Zone-4 and Zone-5) (Stojanovic et al. 2022). The Atlantic Multidecadal Oscillation (AMO) is also one of the indices associated with changes in rainfall patterns (Enfield et al. 2001). The AMO index has been strongly associated with the annual rainfall in the northern half of Ethiopia, including the upper Blue Nile basin (dominantly Zone-1 and Zone-3) during the periods 1951–1965 and 1996–2000, but the association has been weak in the southern region (dominantly Zone-4 and Zone-5) (Wagesho et al. 2013). The higher value of the *CV* in low-rainfall areas indicates that there is a higher interannual variation of rainfall in low-rainfall areas than in high-rainfall areas. Because of this high interannual variability, it is difficult to predict water availability in low-rainfall areas (e.g., Asfaw et al. 2018; Fenta et al. 2017).

Results of analyses of spatial trends (Fig. 4) of rainfall revealed that only 22% of the area of the country has experienced both statistically significant ($p < 0.05$) decreasing (about 19%; Zone-1 and Zone-3) and increasing (about 3%; Zone-2 and Zone-5) trends of annual rainfall (Table 1). However, around 27% and 48% of the area of Ethiopia have experienced non-significant decreasing (up to -1.39 mm/yr) and increasing (up to $+1.22$ mm/yr) trends, respectively, during the period 1901–2020. The greatest of these non-significant decreasing trends of annual rainfall were observed in Zone-1 and Zone-3. The trend of annual rainfall in most areas of Zone-2 and Zone-5 has been increasing but non-significant. The area in both of these zones where the trend was decreasing but non-significant accounted for only 0.09% of the total area of the country during the study period (Fig. 4). Unlike other zones, the areas of non-significant decreasing and increasing annual rainfall trends in Zone-4 were similar and accounted for 17% and 16% of the area of the country, respectively (Table 1). Less than 5% of the area of Ethiopia has not experienced any decreasing or increasing trends in annual rainfall for the last 120 years.

Temporally, the annual rainfall in Zone-1 and Zone-3 decreased at a non-significant rate of 0.38 mm and 0.52 mm per year, respectively, whereas the rainfall in Zone-2

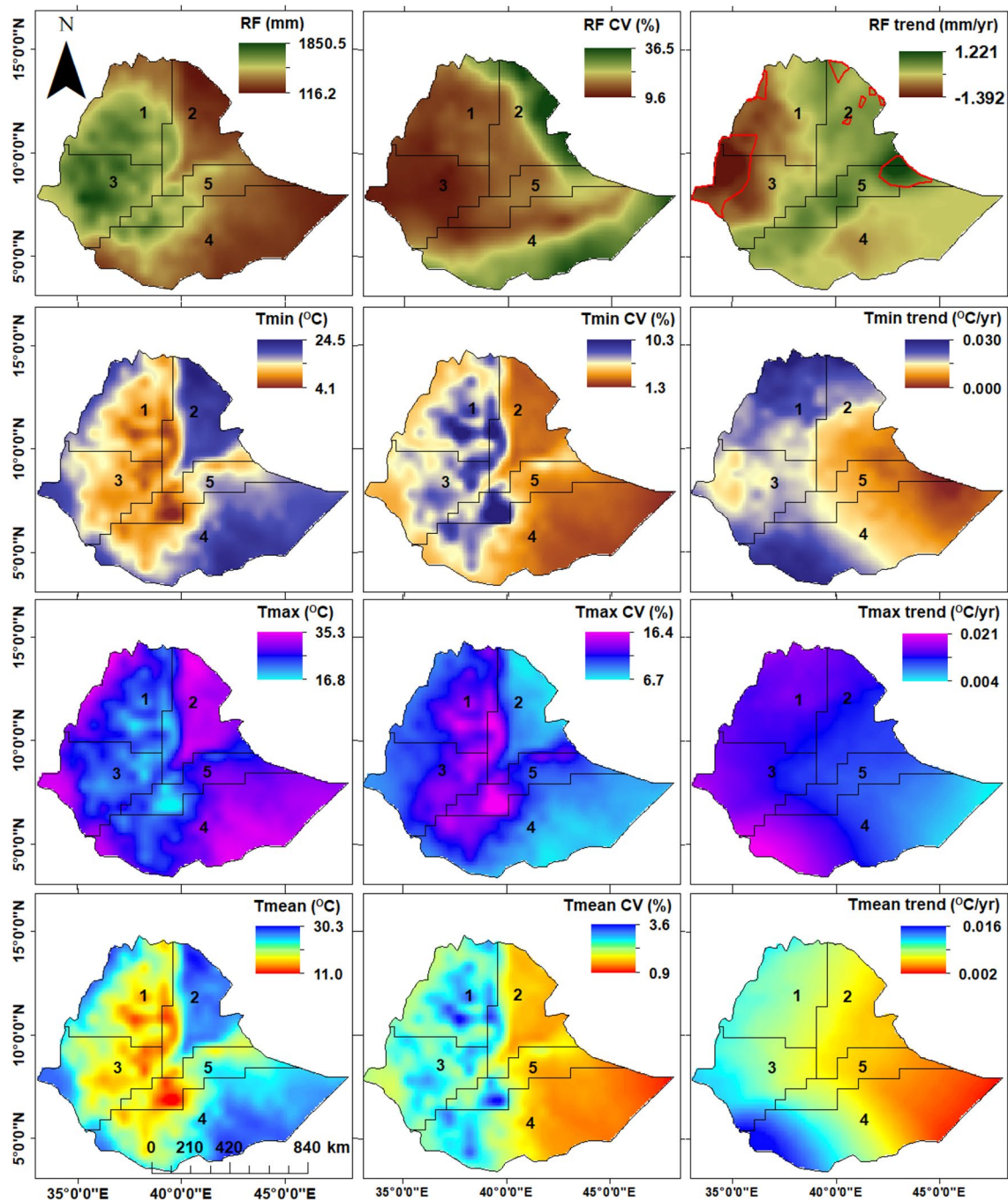


Fig. 4 Spatial distribution of annual rainfall (RF), minimum temperature (Tmin), maximum temperature (Tmax), and average temperature (Tmean) during the period 1901–2020: mean value (left side),

coefficient of variation (CV, middle), and trend (rate of change; right side). Red outlined areas in the upper right panel represent statistical significance areas at $\alpha = 0.05$

(0.24 mm), Zone-4 (0.07 mm), and Zone-5 (0.45 mm) increased with time during the study period (Fig. 5). However, the long-term monotonic trends were not statistically significant with Z_c of -1.30 , 1.08 , -1.61 , 0.29 , and 1.35 for Zone-1, Zone-2, Zone-3, Zone-4, and Zone-5 rainfall, respectively (Table 2, Fig. 5). Likewise, the fact that annual rainfall was highly homogenous in all rainfall

zones indicated that annual rainfall did not change significantly over the 120 years. Hence, we did not reject the null hypotheses of H_0^a and H_0^b for the MK and Pettitt's tests, respectively, for the trends of annual rainfall in all rainfall zones (Table 2, Fig. 5).

Despite the statistically significant spatial increasing and decreasing trends in some parts of Ethiopia (22% of

Table 1 Areal contributions of positive and negative trends and the statistical significance ($\alpha = 0.05$) thereof in annual rainfall for each rainfall zone aggregated from spatial analysis during the study period (1901–2020)

Zone	SA	CV	Annual rainfall trend distribution area contribution							
			Negative		Positive		No change		Trend @ $\alpha = 0.05$	
			(10 ³ km ²)	%	(10 ³ km ²)	%	(10 ³ km ²)	%	(10 ³ km ²)	%
1	1077.13	14.77	163.62	14.33	58.28	5.1	–	43.73	8.43*	
2	556.09	22.44	0.86	0.08	190.36	16.67	–	16.68	3.22*	
3	1343.38	11.68	157.83	13.82	430	3.77	–	34.62	6.67*	
4	544.60	21.5	196.15	17.18	177.67	15.56	35.73	3.13	14.58	2.48**
5	884.07	17.27	0.12	0.01	118.04	10.34	–	4.18	0.71**	
Total			518.58	45.42	974.35	51.44	35.73	3.13	113.79	21.51

*Negative (decreasing) and **positive (increasing) trends. SA: spatial average; CV: mean coefficient of variation

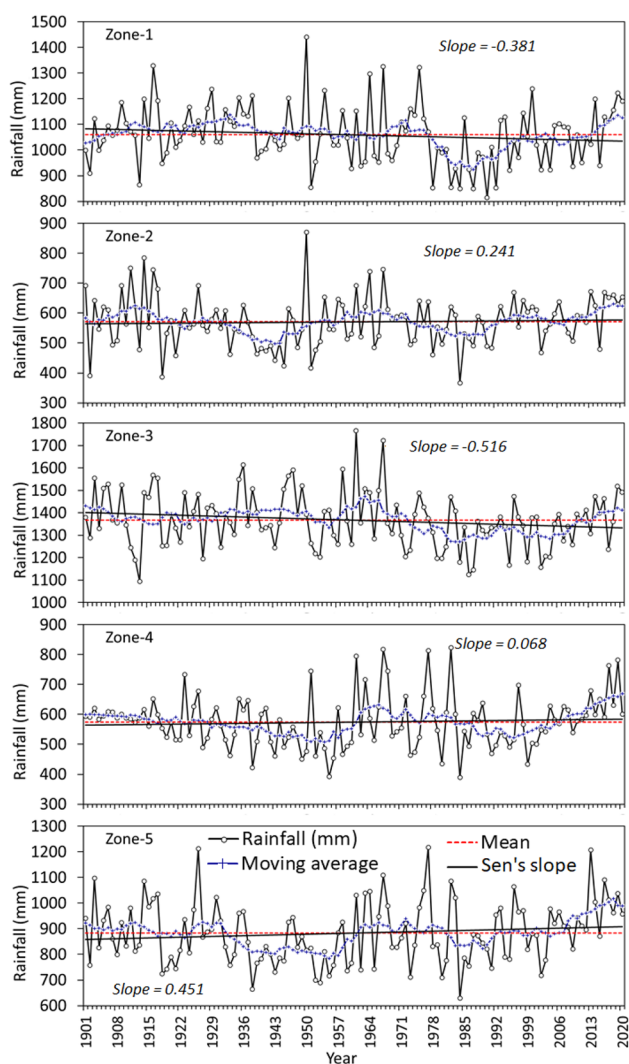


Fig. 5 Trends and changes in annual rainfall in five climate zones from 1901 to 2020. The dotted lines indicate the Pettitt test homogeneity trend result at a significance level $\alpha = 0.05$. Red dashed line shows the mean value of annual rainfall. The black solid lines indicate Sen's slope for the trend

the area), there were no statistically significant spatiotemporal trends of annual rainfall in the country during the study period. The spatiotemporal trend results of this study were consistent with the results of previous studies (Abebe et al. 2022; Alemu and Bawoke 2020; Asfaw et al. 2018; Cheung et al. 2008; Gurara et al. 2022; Jury and Funk 2013; Mengistu et al. 2014; Mulugeta et al. 2019; Tekleab et al. 2013; Wagesho et al. 2013). For example, Wagesho et al. (2013) reported a significant decreasing trend in annual rainfall in the northwestern and western parts of the country (Zone-1 and Zone-3), whereas the annual rainfall in small areas in the east (Zone-2 and Zone-5) increased during the period 1951–2000. However, within 77% of the area of Ethiopia (75% reported in this study), there was no significant trend of annual rainfall during the study period (1951–2000; Wagesho et al. 2013). For example, Abebe et al. (2022) have reported non-significant decreasing and increasing trends of annual rainfall at 51% and 48% of 43 stations in the Tekeze River basin; they observed significant trends at only four stations. A statistically significant trend of annual rainfall has also been reported at quite a few stations in the Woleka Subbasin (located in Zone-1) of Ethiopia (Asfaw et al. 2018). In contrast, even at a 10% significance level, significant decreasing or increasing trends have not been observed in the Amhara region (Alemu and Bawoke 2020). According to Mengistu et al. (2014), there was no significant trend in annual rainfall in 88% of the upper Blue Nile River basin (most parts of Zone-1 and Zone-3) from 1981 to 2010. Other previous research results such as those of Tekleab et al. (2013) in the upper Blue Nile River basin and Mulugeta et al. (2019) in the Awash River basin (most parts of Zone-2 and Zone-5) have not revealed statistically significant decreasing or increasing trends in annual rainfall during the periods of study. In general, it is difficult to track trends of annual rainfall in Ethiopia because of interannual variability and differences in sources of rainfall (e.g., Alhamsry et al. 2019; Degefu et al. 2017; Korecha and Barnston 2007; Mengistu et al. 2014; Seleshi and Zanke 2004).

Table 2 Monotonic trend (Mann–Kendall) test and significant change (Pettitt's homogeneity) test for annual climate variables (Rainfall, Tmin, Tmax, and Tmean) from 1901 to 2020 in five rainfall zones of Ethiopia

Climate variable	Zone	Mann–Kendall test			Sen's slope			Pettitt's test			
		Zc	P	H ₀ ^a	S	Lb (95%)	Ub (95%)	K	P	CP	H ₀ ^b
Rainfall	1	−1.30	0.192	A	−0.381	−0.964	0.209	941.00	0.143	—	A
	2	1.08	0.281	A	0.241	−0.219	0.665	810.00	0.329	—	A
	3	−1.61	0.107	A	−0.516	−1.171	0.095	1052.00	0.063	—	A
	4	0.29	0.773	A	0.068	−0.363	0.456	805.00	0.337	—	A
	5	1.35	0.176	A	0.451	−0.191	1.100	882.00	0.209	—	A
Min. Temperature	1	8.03	< 0.0001	R	0.011	0.009	0.013	2889.00	< 0.0001	1975	R
	2	6.12	< 0.0001	R	0.007	0.005	0.009	2410.00	< 0.0001	1976	R
	3	8.23	< 0.0001	R	0.011	0.009	0.013	3157.00	< 0.0001	1975	R
	4	6.51	< 0.0001	R	0.007	0.005	0.009	2383.00	< 0.0001	1975	R
	5	6.04	< 0.0001	R	0.006	0.004	0.008	2237.00	< 0.0001	1975	R
Max. Temperature	1	3.24	0.001	R	0.005	0.002	0.009	2084.00	< 0.0001	1996	R
	2	2.64	0.008	R	0.004	0.001	0.007	2158.00	< 0.0001	1996	R
	3	4.15	< 0.0001	R	0.007	0.004	0.010	2354.00	< 0.0001	1978	R
	4	5.28	< 0.0001	R	0.007	0.004	0.009	2154.00	< 0.0001	1994	R
	5	3.47	0.001	R	0.004	0.002	0.007	2168.00	< 0.0001	1994	R
Mean Temperature	1	6.03	< 0.0001	R	0.008	0.006	0.011	2625.00	< 0.0001	1975	R
	2	5.44	< 0.0001	R	0.006	0.004	0.008	2493.00	< 0.0001	1975	R
	3	6.70	< 0.0001	R	0.009	0.007	0.011	3017.00	< 0.0001	1975	R
	4	6.52	< 0.0001	R	0.007	0.005	0.008	2200.00	< 0.0001	1986	R
	5	5.66	< 0.0001	R	0.006	0.004	0.007	2279.00	< 0.0001	1989	R

H₀^a is the null hypothesis that there is no monotonic trend in the time series for annual climate variables; H₀^b is the null hypothesis that there is no significant change in the time series data for annual climate variables (the data are homogeneous). The null hypotheses are accepted (A) or rejected (R) at significance level $\alpha=0.05$. S: Sen's slope; CP: change point (inflection point); Lb and Ub: lower and upper bound of Sen's slope, respectively

3.2.2 Inter-seasonal spatial and temporal variability and trend of rainfall

The analysis of spatial variability, temporal trends, and the percentage contribution of seasonal rainfall [Winter (DJF), spring (MAM), summer (JJA), and autumn (SON)] in each rainfall zone for 120 years are briefly described here (Figs. 6, 7, and FS2). The winter season (DJF) includes the driest months in Ethiopia and contributed less than 10% of the annual rainfall in all rainfall zones (Fig. FS2). Also, the mean seasonal rainfall in all zones was lowest during the winter. The spatially averaged rainfall ranged from 21 mm ±17 mm in Zone-1 to 66 mm ±27 mm in Zone-3. However, the southwestern (most parts of Zone-3 and Zone-5) part of Ethiopia received maximum rainfall during the winter (DJF), whereas other parts of the country received low rainfall (Fig. 6). The southern and southeastern parts of Ethiopia (Zone-4, and part of Zone-3 and Zone-5) received maximum rainfall in the spring (MAM) (Fig. 6). Zone-4 and Zone-5 have also received about 48% and 33%, respectively, of their annual rainfall during the spring (Fig. FS2). The average seasonal rainfall was minimum (131 mm ±78 mm) in Zone-2 during

the spring. That amount of rainfall was about twice the maximum mean seasonal rainfall (66 mm ±27 mm) during the winter (DJF) in Zone-3. The spatial distribution of mean summer (JJA) rainfall (also called the major rainy season in Ethiopia, Fig. 6) was greatest over the highlands of western and west-central Ethiopia (Zone-1, Zone-3, and some parts of Zone-5), whereas the northeast and southeast (Zone-2, and parts of Zone-4 and Zone-5) lowlands were relatively dry (Fig. 6). Summer rainfall contributed 65% in Zone-1, 53% in Zone-2, and 49% in Zone-3 of the total annual rainfall (n.b., more than 50% of the summer rainfall occurs during July and August). This seasonality clearly showed that rainfall was highly concentrated during the summer (Fig. FS2). The mean summer rainfall ranged from 62 mm ±80 mm in Zone-4 to 700 mm ±150 mm in Zone-1. Autumn rainfall (SON) contributed 17% to Zone-2 and 33% to Zone-4 of the annual rainfall (Fig. FS2). In addition to MAM rainfall, the south and southeastern part of Ethiopia (Zone-4) received high rainfall during autumn (SON) (Fig. 6).

Seasonal rainfall was characterized by high interannual variability compared to annual rainfall, up to 134% in the case of DJF rainfall; the average CV of this season varied

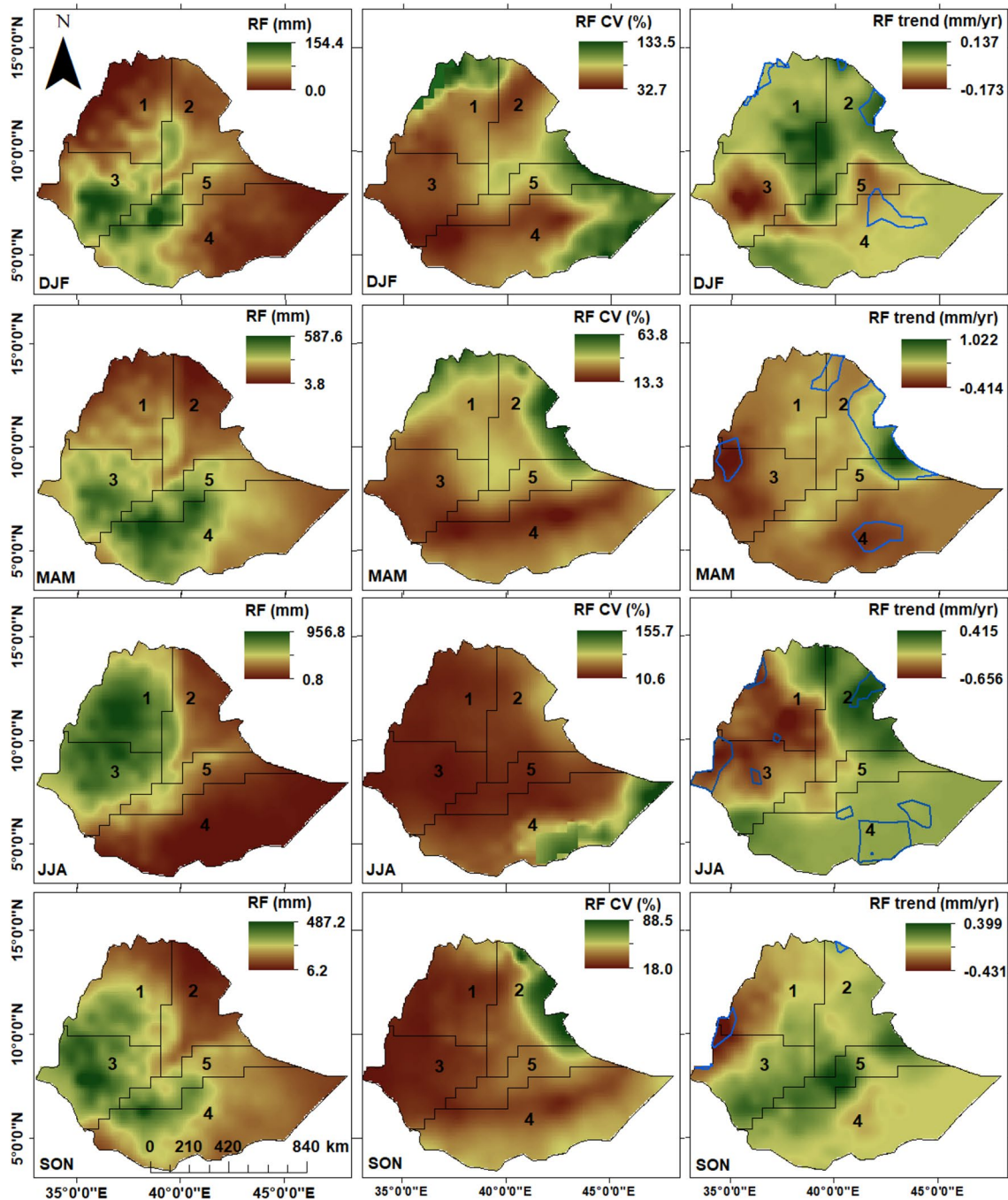


Fig. 6 Spatial distribution of seasonal rainfall (RF) during the period 1901–2020: mean value (left side), coefficient of variation (CV, middle), and trend (rate of change in mm/yr; right side). Blue-coloured

outlined areas represent statistical significance areas at $\alpha = 0.05$. DJF, December–January–February; MAM, March–April–May; JJA, Jun–July–August; SON, September–October–November

from $48\% \pm 8\%$ in Zone-3 to $71\% \pm 18\%$ in Zone-5 during the study period (Fig. 6). The CV of JJA rainfall was comparatively small compared to the other seasons (except in Zone-4 during JJA, when it was as much as 156%); the average CV in each rainfall zone was less than 20%, except in Zone-2 (33%) and Zone-4 (43%). The CV was a maximum in the northwestern (part of Zone-1), eastern (parts of Zone-2 and

Zone-5), and southeastern (part of Zone-4) parts of the country (Fig. 6) during the winter (DJF rainfall). In MAM, the CV of rainfall was a maximum in the eastern (part of Zone-2 and -5), northeastern (Zone-2), and northwestern (part of Zone-1) parts of Ethiopia. However, in JJA and SON, the CVs were highest in the northeastern (part of Zone-4) and eastern (part of Zone-2) parts of Ethiopia (Fig. 6).

Unlike annual rainfall, the *CV* of seasonal rainfall was high. Hence, there was much larger interannual variability in seasonal rainfall. This conclusion is consistent with the results of previous studies in different parts of Ethiopia, for example, Abebe et al. (2022) in the Tekeze-Atbara River basin (Zone-1), Asfaw et al. (2018) in Mekaneslam (located in Zone-1), Cheung et al. (2008) in 13 watersheds in different parts of Ethiopia, Mewded et al. (2022) in Lake Hayk (on the border of Zone-1 and Zone-2), and Seleshi and Zanke (2004) at 11 meteorological stations throughout Ethiopia (all zones). These studies have reported that the variability of seasonal rainfall is very low and high during the summer (JJA) and winter (DJF), respectively. However, the summer (JJA) rainfall varies greatly from year to year, both in timing and total amount. This great variability may be attributed to the variation in direction and magnitude of the summer monsoon (Inter-tropical Convergence Zone, ITCZ), tropical upper easterlies; local convergence in the Red Sea coastal region; and El Niño–Southern Oscillation (ENSO, an irregular seasonal variation in winds and sea surface temperatures over the tropical eastern Pacific Ocean) in each season (Broman et al. 2020; Conway 2000; Degefu et al. 2017; Diro et al. 2011; Gleixner et al. 2017; Korecha and Barnston 2007; Seleshi and Camberlin 2006). For example, summer rainfall has been found to be influenced by ENSO. The most significant effects occur over the northern half of Ethiopia, but there are no effects in the Ethiopian Rift Valley or along the Eastern Escarpment (Zone-2 and Zone-5) (Conway 2000; Korecha and Barnston 2007). Likewise, because of the elevated topographic terrain over the central part of Ethiopia, a moisture flux is produced during summer (JJA) in most parts of the country because of the movement of the low-pressure ITCZ to northern Ethiopia (Conway 2000; Degefu et al. 2017). Alternatively, during the spring (MAM), the meridional arm of the ITCZ produces rainfall over southwestern (parts of Zone-3 and Zone-4) Ethiopia because of the variation in heat flux between the Indian Ocean and the land surface (Degefu et al. 2017). The summer is very important for agricultural production and major societal operations (e.g., hydropower generation, irrigation, and drinking water) in most parts of Ethiopia. Farmers may be unable to mitigate the negative effects of such climate variability on crop production, and high seasonal variability in the summer thus leads to crop failures (Abebe et al. 2022; Alemu and Bawoke 2020; Korecha and Barnston 2007).

An analysis of the spatial patterns of seasonal rainfall from 1901 to 2020 showed decreasing and increasing temporal trends but with considerable spatial variations (Fig. 6 and Table TS1, TS2). As a result, spatially, the seasonal rainfall decreased and increased up to -0.66 mm per year in summer (JJA) and 1.02 mm per year in spring (MAM), respectively (Fig. 6). However, only 9%, 26%, 25%, and 4% of the area of the country during winter, spring, summer, and autumn have

shown both statistically significant ($\alpha < 0.05$) decreasing and increasing trends of seasonal rainfall (Fig. 6 and Table TS1). In contrary, during the summer, large areas of the country (70% of the area of Ethiopia) experienced a non-significant trend of decreasing seasonal rainfall that far exceeded the areal contribution of other seasons, which ranges from 35% in autumn to 50% in winter over the study period (Table TS1). In all seasons except autumn, the real contribution of the non-significant spatial trend of decreasing rainfall in Zone-4 exceeded the areal contribution of other rainfall zones. In contrast, 30% (summer) to 59% (autumn) of the area of the country experienced a non-significant trend of increasing seasonal rainfall (Table TS1). Compared to other rainfall zones, large areas experienced a trend of increasing seasonal rainfall in Zone-4 during the winter (4%) and summer (16%) and in Zone-3 during spring (9%) over the study period (Fig. 6 and Table TS1). Generally, unlike annual rainfall, more decreasing and increasing trends of seasonal rainfall have been observed in all rainfall zones.

The temporal trends in seasonal rainfall shown in Fig. 7 and Table TS2 indicate a non-significant increase (Zones-1 and Zone-2), and decrease (Zones-3, Zone-4, and Zone-5) of seasonal rainfall during the winter. In the spring, there was a non-significant, increasing trend of rainfall in all rainfall zones except Zone-3 (Fig. 7). However, during the summer, there was a non-significant decreasing trend of rainfall in all rainfall zones except Zone-4. Likewise, the seasonal rainfall decreased in Zone-1, Zone-2, and Zone-3 and increased in Zone-4 and Zone-5 during the autumn (Fig. 7, Table TS2). Generally, there was no significant (at $\alpha = 0.05$) long-term, monotonic trend in rainfall, and there was a strong homogeneity of seasonal rainfall in all rainfall zones except in Zone-3 during the summer (Table TS2). We therefore did not reject the null hypotheses for the MK and Pettitt's tests for seasonal rainfall trends in all rainfall zones (Table TS2). The fact that there was a significant decreasing trend of 0.37 mm per year of long-term seasonal rainfall in Zone-3 during the summer (JJA) indicated that seasonal rainfall changed (the year of the change was 1979) significantly over 120 years (Fig. 7). Similarly, in all rainfall zones, there were significant (at $\alpha = 0.05$) long-term, monotonic trends not apparent in monthly rainfall during all months except April (Zone-2), June (Zone-3), and October (Zone-2, Zone-3, and Zone-5) (Table TS2).

Statistically non-significant but increasing and decreasing trends of seasonal rainfall in this study agreed with those found in previous studies conducted in Ethiopia (e.g., Abebe et al. 2022; Alemu and Bawoke 2020; Mengistu et al. 2014; Mulugeta et al. 2019). For example, a study in the Upper Blue Nile basin (part of Zone-2 and Zone-3) by Mengistu et al. (2014) revealed statistically non-significant increasing trends of rainfall in winter, summer, and spring, whereas rainfall trended downward during the autumn. Although significant

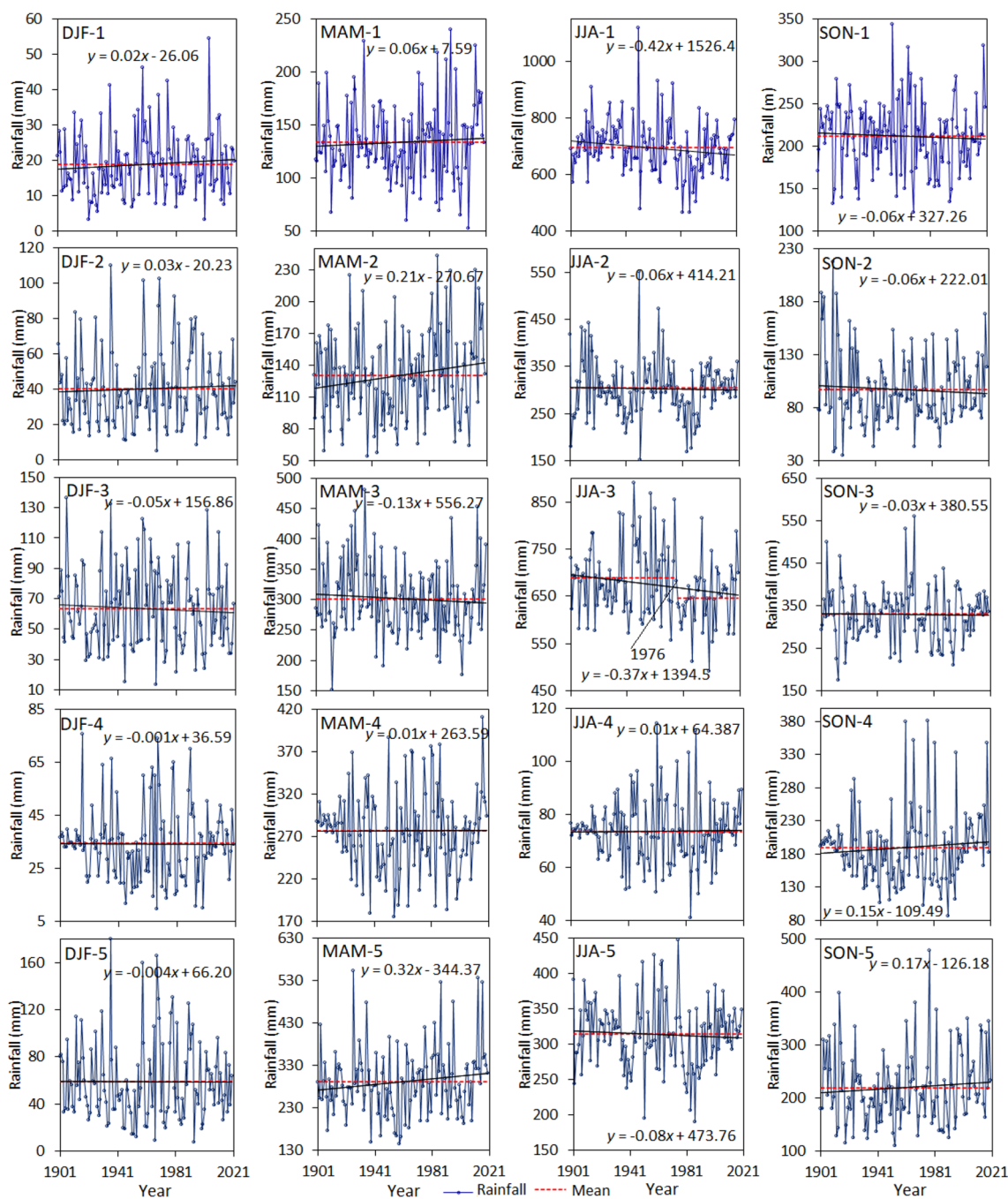


Fig. 7 Trends and changes in seasonal rainfall in five climate zones of Ethiopia from 1901 to 2020. The dashed lines indicate the Pettitt test homogeneity trend result at a significance level $\alpha=0.05$ and show the

mean value of seasonal rainfall before and after the inflection point. DJF, December-January-February; MAM, March-April-May; JJA, Jun-July-August; SON, September-October-November

decreasing and increasing trends of seasonal rainfall was apparent in some areas of the study (Fig. 6), our temporal trend analyses in different parts of rainfall zones revealed that seasonal rainfall did not display any significant changes over the study period, except in Zone-3 during the summer (Fig. 7). Like our spatial trend analysis results, Wagesho et al. (2013) found significant decreasing trends in seasonal rainfall

from 1951–2000 in northwestern and western parts of Ethiopia (corresponding to Zone-1 and Zone-3), whereas seasonal rainfall trended upward in a small area in the east (corresponding to Zone-2 and Zone-5). The temporal decreases in seasonal rainfall in Zone-3 during the summer (Fig. 7) also agreed with a study conducted by Cheung et al. (2008), who stated that watersheds located in southwestern Ethiopia

(corresponding to Zone-3) experienced a significant decrease in summer rainfall. A rainfall variability and trend analysis based on 43 selected rainfall stations in the Tekeze-Atbara River basin in northwestern Ethiopia by Abebe et al. (2022) revealed significant increasing and decreasing trends of rainfall in the summer, but those trends were apparent at only on three rainfall stations. Another study by Mulugeta et al. (2019) in the Awash River basin (part of Zone-2 and Zone-5) revealed that the summer rainfall trended downward significantly, whereas the trends of winter and spring rainfall were not significant from 1902 to 2016. A worldwide review by Easterling et al. (2000) has revealed a significant decreasing trend of rainfall in the summer (JJA) of 11.6% between 1950 and 1987 in Ethiopia. It is important to note that comparing the results of this study with some previous studies is a bit complicated for several different reasons. There is also evidence that contradictions in the results of climate research in Ethiopia are associated with data sources, data quality, the period of the study, and the spatial extent of the study area (e.g., Abebe et al. 2022; Cheung et al. 2008). It is also difficult to compare these studies because, to the authors' knowledge, only a limited number of such studies have been conducted in Ethiopia on a national scale.

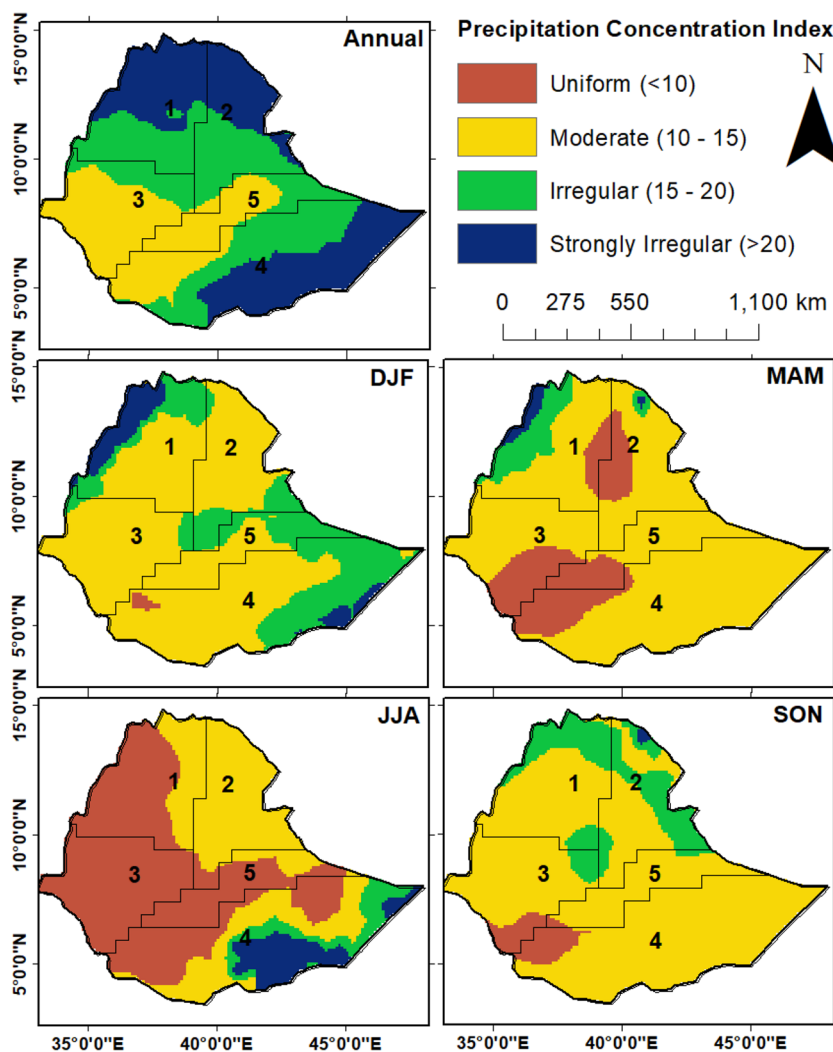
3.2.3 The spatial and temporal pattern of rainfall indices across rainfall zones

The long-term PCI spatial analysis results showed that the country exhibited moderate (28%), irregular (38%), and strongly regular (34%) annual rainfall distributions (Fig. 8). The indication was that rainfall was highly seasonal throughout the year. The most extensive seasonality (highly irregular annual rainfall distribution) of rainfall was apparent in Zone-1 (56% of the area), followed by Zone-2 (46% of the area) and Zone-4 (44% of the area) (Fig. 8 and Table TS3). However, in Zone-3 and Zone-5, annual rainfall was moderately distributed over more than 70% of the area during the study period (Table TS3). In contrast, the SPCI analysis revealed that seasonal rainfall was moderately distributed (mean SPCI = 10–15, Fig. 8 and Table TS3) over large parts of areas that accounted for 56% of Zone-1 to 93% of Zone-3 in winter (DJF), 59% of Zone-1 to 84% of Zone-3 in spring (MAM), 57% of Zone-2 to 92% of Zone-3 in autumn (SON), and 94% of the area of Zone-2 during the summer (JJA). In contrast, 67%, 100%, and 75% of the areas of Zone-1, Zone-3, and Zone-5, respectively, were characterized by a uniform seasonal rainfall distribution during the summer (JJA) (mean SPCI = below 10, Fig. 8 and Table TS3). Strongly seasonal, irregular distributions (mean SPCI = above 20) of rainfall (~20% of the area) were apparent during the winter and summer in Zone-1 and Zone-4, respectively (Fig. 8 and Table TS3).

The distribution of rainfall was irregular during 96 and 79 out of 120 years in Zone-1 and Zone-2, respectively (Table 3). Irregular rainfall distribution is often linked to climate change, which can alter weather patterns. If climate change intensifies, irregular rainfall distribution may become more frequent, leading to longer dry spells, more intense rainfall events, and increased weather extremes in these zones (e.g., Moreno and Møller 2011). In contrast, Zone-3, Zone-4, and Zone-5 experienced moderate rainfall distributions during 114, 68, and 115 out of 120 years, respectively (Fig. 9 and Table 3). The distributions of rainfall in the remaining years in the three zones were irregular (mean SPCI = 15–20, Fig. 9, and Table 3). In all rainfall zones, the seasonal distributions of rainfall were uniform and moderate during the winter, spring, and autumn (only Zone-3, Zone-4, and Zone-5) during more than 100 of the 120 years (Table 4, Fig. FS3). Likewise, the seasonal distribution of rainfall was uniform in all zones except Zone-2 (which experienced moderate rainfall distributions for 95 years) during the summer during 110 years from 1901 to 2020 (Table 4, Fig. FS3). The seasonal distribution of rainfall was more temporally irregular in Zone-1, Zone-2, and Zone-5 during the winter (Table 4, Fig. FS3). The contrasting results obtained from PCI and SPCI can be primarily attributed to the amount and variability in annual and seasonal rainfall in the study area. Moreover, it is worth noting that the variation in rainfall among seasons is typically more pronounced than that of annual rainfall.

We selected only the top three excess years (1916, 1967, and 2019: SPI > 1) and three most deficient years (1902, 1984, and 2002: SPI < -1) for detailed spatial analysis (Fig. 10 and Table TS4) based on the distribution of anomalies over the rainfall zones. Most of the deficit or excess rainfall years were local phenomena. The severe drought of 1984 has been regarded as the cause of a widespread Ethiopian famine (Fig. 10). There was little rainfall in the summer of 1984, and more than 94% of the areas of each zone experienced dry (-1 to -1.5) to extremely dry (< -2) rainfall conditions (Fig. 10, Table TS4). In that year of severe drought, only Zone-1 and Zone-3 (about 30% of the area of each zone) experienced normal rainfall (-1 < SPI < 1, Fig. 10, Table TS4). Some parts of rainfall zones were also exposed to dry to extremely dry rainfall conditions during 1902 and 2002. In contrast, rainfall conditions were wet (SPI = 1 to 1.5) to extremely wet (> 2) during 1967 in more than 80% of the area of each rainfall zone (Fig. 10, Table TS4). The time series of annual SPI metrics revealed that the number of excess and deficit years (15 to 20 years, respectively) that occurred across the rainfall zones were nearly equal (Table 3). With some exceptions, rainfall conditions were normal (SPI between -1 and 1) during more than 80 years (Fig. 11, Table 3). The highest positive anomalies (SPI =

Fig. 8 Spatial distribution of the mean annual and seasonal precipitation concentration index (PCI) during the period 1901–2020. DJF, December–January–February; MAM, March–April–May; JJA, June–July–August; SON, September–October–November



2.8–3.6) occurred in the years 1950 (Zone-1, Zone-2, and Zone-3), 1982 (Zone-4), and 1977 (Zone-5). The most negative anomalies ($SPI = -2.0$ to -2.4) occurred in 1984 in all rainfall zones (Fig. 11).

Both the seasonal and annual SPI values indicated that rainfall conditions were normal during more than 80 years in all rainfall zones. There were fewer than 20 out of 120 years during which there was an excess or deficit of rainfall (Fig. FS4 and Table 5). There was a predominance of negative anomalies (more deficits) during the winter (DJF) in Zone-1 and Zone-2, whereas those anomalies occurred mainly in the spring (MAM) in Zone-4 and Zone-5 (Table 5 and Fig. FS4). Excess rainfall occurred primarily during the winter (Zone-3), spring (Zone-1 and Zone-3), and autumn (Zone-5). The results of this study can be used to complement the non-significant trends in annual and seasonal rainfall in the study area (Figs. 5 and 7). The fact that the number of positive and negative seasonal rainfall anomalies exceeded the number of annual anomalies suggested that in Ethiopia inter-seasonal rainfall variability was higher than annual rainfall variability

(Figs. 11 and FS4). Given the difference in the frequency of occurrence of droughts among rainfall zones, Ethiopia was exposed to meteorological droughts for a number of 10 to 20 years from 1901 to 2020 (Tables 3 and 5). The highest positive and negative anomalies occurred in different years as a function of the seasons and rainfall zones (Fig. FS4). In all rainfall zones except Zone-4, negative anomalies (52% to 54%) slightly outnumbered positive anomalies (46% to 48%) at an annual timescale (Table 5). The percentage of negative anomalies exceeded the percentage of positive anomalies during all seasons except summer in Zone-5 and autumn in Zone-1 and Zone-3 (Fig. FS4 and Table 5). In general, the annual and seasonal SPI values reflected the interannual and seasonal variations of the distribution of rainfall across the rainfall zones of Ethiopia.

The changes that we documented in the distribution of rainfall and the occurrence of drought years in Ethiopia agreed with previous studies conducted at local and national scales in Ethiopia (e.g., Asfaw et al. 2018; Belay et al. 2021; Mewded et al. 2022). Those studies have also reported a

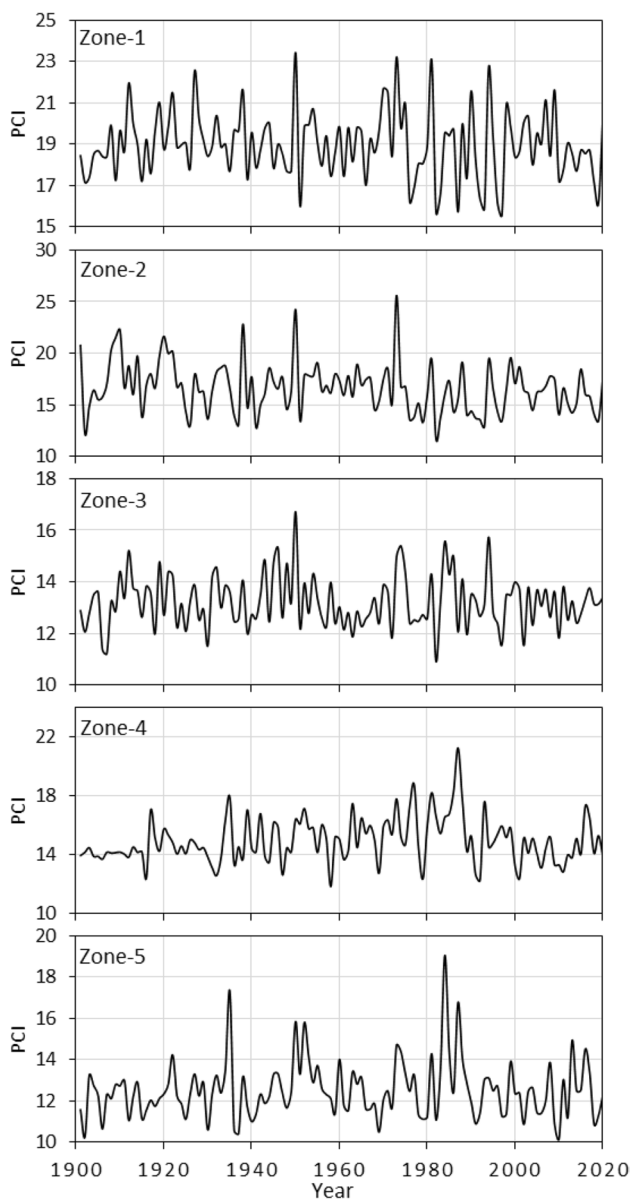


Fig. 9 Annual precipitation concentration index (PCI) from 1901 to 2020 across the five climate zones of Ethiopia

higher percentage of negative anomalies than positive anomalies. The drought years have been associated with El Niño events and sea surface temperature (e.g., Alhamshry et al. 2019; Belay et al. 2021; Bayable et al. 2021; Diro et al. 2011; Gleixner et al. 2017). For example, in parts of southern Ethiopia (from 1983 to 2016, Belay et al. 2021) and eastern Ethiopia (from 1983 to 2019, Bayable et al. 2021), the drought and wet years were associated with El Niño and La Niña events, respectively. During the 1984 drought year, Ethiopia as well as East Africa also suffered from low rainfall because of an El Niño event that affected all seasons (Diro et al. 2011; Viste et al. 2013). Moreover, severe drought years during the period 1965–2002 corresponded to

the highest negative rainfall and positive sea surface temperature anomalies reported by Seleshi and Camberlin (2006). It is important to note that the positive and negative rainfall anomalies are important indicators of water availability for planning water resource management in a given area. Incorporating this information into water management planning will facilitate improved crop production and enhance the livelihoods of the people who farm the land.

3.3 Spatiotemporal variability and trend of temperature

3.3.1 Inter-annual spatiotemporal variability and trend of temperature

The spatial distribution of T_{min} , T_{max} , and T_{mean} of Ethiopia ranged from about 4 °C to 25 °C, 17 °C to 35 °C, and 11 °C to 30 °C, respectively from 1901 to 2020 (Fig. 4). The spatial averages of T_{min} were similar in Zone-1 and Zone-3 ($14^{\circ}\text{C}\pm 3^{\circ}\text{C}$, western Ethiopia) as well as in Zone-2 and Zone-4 ($18^{\circ}\text{C}\pm 5^{\circ}\text{C}$, south and east parts of Ethiopia). The spatial averages of T_{max} ($26^{\circ}\text{C}\pm 4^{\circ}\text{C}$) and T_{mean} ($20^{\circ}\text{C}\pm 4^{\circ}\text{C}$) were likewise similar in two rainfall zones (Zone-3 and Zone-5) during the study period. The T_{max} and T_{mean} were 1 °C higher in Zone-1 than in Zone-3 and Zone-5. The spatial averages of T_{max} ($30^{\circ}\text{C}\pm 5^{\circ}\text{C}$) and T_{mean} ($24^{\circ}\text{C}\pm 3^{\circ}\text{C}$) were similar in Zone-2 and Zone-4 (Fig. 4). The interannual variability of temperature could be quantified in terms of the CV of temperature in each rainfall zone. The CVs of T_{min} , T_{max} , and T_{mean} in Ethiopia varied from approximately 1–10%, 7–16%, and 1–4%, respectively (Fig. 4). More interannual variability of T_{min} ($CV = \sim 4\% \pm 1\%$), T_{max} ($CV = \sim 11\% \pm 1.5\%$), and T_{mean} ($CV = \sim 2.5\% \pm 0.3\%$ except for Zone-5) were observed in Zone-1, Zone-3, and Zone-5 during the study period (Table TS5). The interannual variability of T_{max} has generally been high across all rainfall zones, followed by T_{min} and T_{mean} (Fig. 4, Table TS5). This pattern indicates that there is less variation of temperature at low temperatures than at high temperatures.

Unlike annual rainfall, there was a statistically significant increasing trend of annual temperature (T_{min} , T_{max} , and T_{mean}) in all rainfall zones (Fig. 4). From 1901 to 2020, T_{min} increased significantly by 1.32 °C in Zone-1 and Zone-3, by 0.84 °C in Zone-2 and Zone-4, and by 0.72 °C in Zone-5. Similarly, from 1901 to 2020 the increases of annual T_{max} and T_{mean} in Ethiopia ranged from 1.32 °C (Zone-4 and Zone-5) to 1.80 °C (Zone-1) and from 0.72 °C (Zone-2, Zone-4, and Zone-5) to 1.08 °C (Zone-3), respectively (Table TS5). Generally, in Ethiopia, the T_{mean} increased by 0.24 °C to 1.92 °C over the study period (Fig. 4). Like the spatial patterns of the temporal trends of temperature, the significant (at $\alpha = 0.05$) monotonic temporal trends in

Table 3 The number of years (# Yrs) and their occurrence (%) for the annual precipitation concentration index (PCI) and the standard precipitation anomaly index (SPI) for each rainfall zone (Zone-1 to Zone-5) between 1901 and 2020

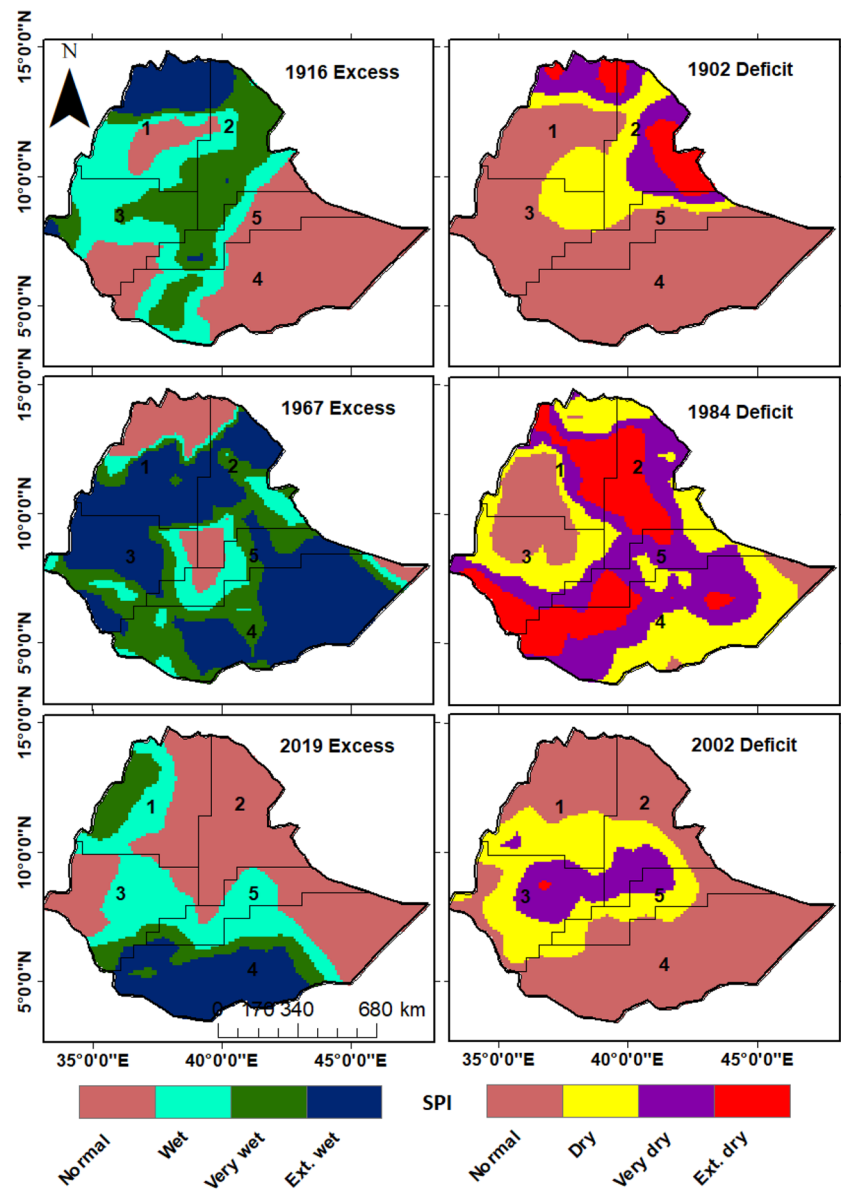
Rainfall distribution	PCI	Zone-1		Zone-2		Zone-3		Zone-4		Zone-5	
		#Yrs	(%)	#Yrs	(%)	#Yrs	(%)	#Yrs	(%)	#Yrs	(%)
Uniform	below 10	0	0	0	0	0	0	0	0	0	0
Moderate	10 to 15	0	0	32	27	114	95	68	57	115	96
Irregular	15 to 20	96	80	79	66	6	5	51	43	5	4
Strongly irregular	above 20	24	20	9	8	0	0	1	1	0	0
Total		120	100	120	100	120	100	120	100	120	100
Classification		SPI									
Extremely wet	above 2	5	4	5	4	5	4	6	5	3	3
Very wet	1.5 to 2	3	3	1	1	3	3	4	3	6	5
Wet	1.0 to 1.5	9	8	9	8	9	8	3	3	11	9
Normal	-1.0 to 1.0	85	71	86	72	85	71	92	77	80	67
Dry	-1 to -1.5	10	8	13	11	10	8	10	8	16	13
Very dry	-1.5 to -2	7	6	3	3	7	6	3	3	3	3
Extremely dry	below -2	1	1	3	3	1	1	2	2	1	1
Excess	> Normal	17	14	15	13	17	14	13	11	20	17
Deficit	< Normal	18	15	19	16	18	15	15	13	20	17

Table 4 The number of years (# Yrs) and their occurrence (%) under different rainfall distributions with the seasonal precipitation concentration index (SPCI) in each of five climate zones between 1901 and 2020

Rainfall distribution	SPCI	DJF-1		DJF-2		DJF-3		DJF-4		DJF-5	
		#Yrs	(%)	#Yrs	(%)	#Yrs	(%)	#Yrs	(%)	#Yrs	(%)
Uniform	< 10	48	40	30	25	51	43	74	62	39	33
Modrate	10 to 15	61	51	67	56	62	52	41	34	55	46
Irregular	15 to 20	11	9	20	17	5	4	4	3	22	18
Strong irregular	> 20	0	0	3	3	2	2	1	1	4	3
Total		120	100	120	100	120	100	120	100	120	100
		SPCI		MAM-1		MAM-2		MAM-3		MAM-4	
Uniform	< 10	27	23	72	60	63	53	56	47	75	63
Modrate	10 to 15	86	72	48	40	55	46	63	53	42	35
Irregular	15 to 20	7	6	0	0	2	2	1	1	3	3
Strong irregular	> 20	0	0	0	0	0	0	0	0	0	0
Total		120	100	120	100	120	100	120	100	120	100
		SPCI		JJA-1		JJA-2		JJA-3		JJA-4	
Uniform	< 10	111	93	25	21	120	100	117	98	113	94
Modrate	10 to 15	9	8	95	79	0	0	3	3	7	6
Irregular	15 to 20	0	0	0	0	0	0	0	0	0	0
Strong irregular	> 20	0	0	0	0	0	0	0	0	0	0
Total		120	100	120	100	120	100	120	100	120	100
		SPCI		SON-1		SON-2		SON-3		SON-4	
Uniform	< 10	3	3	10	8	27	23	79	66	26	22
Modrate	10 to 15	88	73	65	54	89	74	41	34	89	74
Irregular	15 to 20	29	24	40	33	4	3	0	0	4	3
Strong irregular	> 20	0	0	5	4	0	0	0	0	1	1
Total		120	100	120	100	120	100	120	100	120	100

DJF, December-January-February; MAM, March-April-May; JJA, Jun-July-August; SON, September-October-November

Fig. 10 Spatial distribution of annual standard precipitation anomaly index (SPI) for selected years during the period 1901–2020. The selection was based on the relative occurrence of excess and deficit rainfall in the climate zones



annual temperature (T_{min} , T_{max} , and T_{mean}) in rainfall zones (Table 2 and Fig. 12) confirmed that there were significant changes in temperature between 1901 and 2020. We, therefore, rejected the null hypotheses of H_0^a and H_0^b , respectively, for the MK and Pettitt's tests for annual T_{min} , T_{max} , and T_{mean} trends in all rainfall zones (Table 2). It is important to note that the slope (spatial and temporal) of the trend was similar for T_{min} and T_{mean} in each rainfall zone (Fig. 12, Table TS5). However, the slope of the spatial trend of increasing temperature (0.48–0.84°C per 120 years) was much lower than the temporal trend, particularly in the case of the annual T_{max} (Fig. 4 and 12b). A homogeneity test applied to the annual T_{min} , T_{max} , and T_{mean} indicated an inflection point in the 1970s for T_{min} , T_{max} (only for Zone-3), and T_{mean} (only for Zone-1, Zone-2, and Zone-3), the

1980s for T_{mean} (Zone-4 and Zone-5), and the 1990s for T_{max} (except Zone-3) (Fig. 12, Table 2). This pattern indicates that the inflection point of T_{mean} was strongly influenced by the inflection point of T_{min} in all rainfall zones.

There was less annual variability of temperature in Ethiopia at low temperatures than at high temperatures (i.e., annual variability increased in the order of $T_{mean} < T_{min} < T_{max}$). This interannual variability could be verified by the long-range anomalies (Fig. FS5) of annual temperatures in the study area in each rainfall zone. There have been a limited number of national-scale studies, but the results of this study agreed well with the results of previous local studies conducted in Ethiopia (e.g., Asfaw et al. 2018; Conway et al. 2004; Habte et al. 2021; Mengistu et al. 2014; Mewded et al. 2022; Tekleab

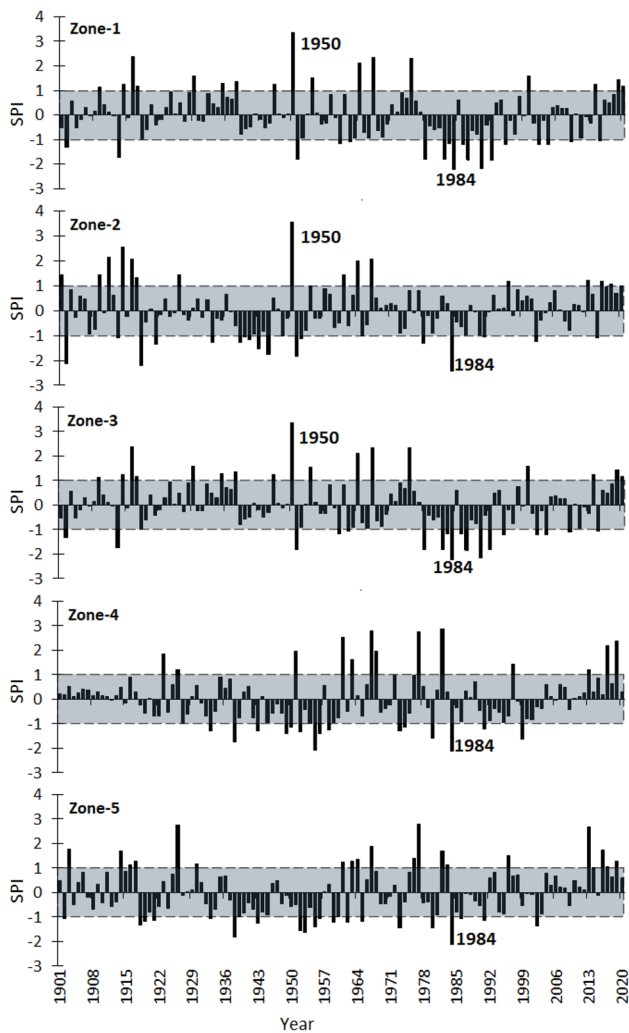


Fig. 11 Annual standardized rainfall anomaly indices for five climate zones from 1901 to 2020 relative to the long-term average of the same period. The shaded area indicates the *SPI* values within the normal condition (-1 to 1)

et al. 2013). For example, a study in the Lake Hayk basin (on the border of Zone-1 and Zone-2) by Mewded et al. (2022) revealed that the annual *Tmean* was less variable than *Tmin* and *Tmax* from 1986 to 2015. In this study, we found that the statistically significant rates of change of temperature varied spatially (Fig. 4) and temporally (Fig. 12). Variations of annual temperature (*Tmin*, *Tmax*, and *Tmean*) have also been reported in previous studies conducted at local and national scales (e.g., Belay et al. 2021; Conway et al. 2004; Habte et al. 2021; Jury and Funk 2013; Mewded et al. 2022). However, the rate of change differs as a function of the location, extent of the study area, and duration of the study. For example, a previous study in the upper Blue Nile basin (most parts of Zone-1 and Zone-3) by Conway et al. (2004) has revealed

that the annual *Tmin* and *Tmax* increased by 0.40 °C and 0.20 °C per decade, respectively, between 1951 and 2002. In that study basin, annual *Tmin* and *Tmax* increased by 0.22 °C and 0.16 °C per decade from 1981 to 2010 (Mengistu et al. 2014). This increasing trend of annual *Tmin* and *Tmax* in the upper Blue Nile basin (Conway et al. 2004; Mengistu et al. 2014) is by far greater than the results of this study, specifically for Zone-1 and Zone-3 (*Tmin* and *Tmax* increased by 0.11 °C and 0.06 °C per decade, respectively, Fig. 12a, b). The increasing trend of *Tmax* and *Tmean*, however, were in reasonable agreement with the previous study conducted in the Woleka sub-basin (part of Zone-1) by Asfaw et al. (2018) during the period of 1901–2014. A study in southern (Zone-4) Ethiopia by Belay et al. (2021) has also revealed that the rate of increase of annual *Tmin*, *Tmax*, and *Tmean* was 0.56 °C, 0.27 °C, and 0.42 °C per decade, respectively. From 1983 to 2016 (34 years), the annual *Tmin* and *Tmax* of southwestern Ethiopia (part of Zone-3 and Zone-4) increased by 0.71 °C and 0.65 °C, respectively (Habte et al. 2021). Importantly, in agreement with the results of our study, a significant increasing trend in *Tmin* (up to 1.2 °C) and *Tmax* (up to 1.9 °C) has been observed in the East Africa region from 1979 to 2010 (Gebrechorkos et al. 2019). It is worth noting that the result of this study (the national average temperature increased by 1.23 °C from 1901 to 2020) was very close to the global warming rate reported in 2020, about 1.2 °C above the pre-industrial (from 1850 to 1900) level (WMO, 2020). Also, like the results of this study, the average global temperatures decreased from 1940 to 1970 (clearly apparent in the *Tmin* of this study, Fig. 12a), and then the temperatures began to climb rapidly again (IPCC 2007). The downward trend from 1940 to 1970 has been attributed mainly to a high concentration of aerosols in the atmosphere emitted by volcanic eruptions and industrial activities during this period (IPCC, 2007). Hence, the change in annual mean temperatures in Ethiopia was linked to the rise of global temperatures after the 1970s. The 1970s and 1990s were the inflection points for *Tmin* and *Tmean*, and *Tmax*, respectively, in all rainfall zones of the study area (Fig. 12). The change of the annual temperatures in the 1970s in Ethiopia was also directly related to the transition of ENSO towards more warm events after the late 1970s and coincided with record-high global mean temperatures (Conway 2000; Dai et al. 1998). It is evident from the long-term trends and anomalies of the annual *Tmax* (Fig. FS5) that there has been a warming trend since the last period of the 20th century (the 1990s). Similar results have also been reported by previous studies in Ethiopia (e.g., Asfaw et al. 2018; Conway et al. 2004; Mengistu et al. 2014; Mewded et al. 2022). Likewise, the global temperatures are projected

Table 5 The number of years (# Yrs) and their occurrence (%) under different classifications and with the standard precipitation anomaly index (SPI) in each of five rainfall zones between 1901 and 2020

Classification	SPI	DJF-1		DJF-2		DJF-3		DJF-4		DJF-5	
		#Yrs	(%)	#Yrs	(%)	#Yrs	(%)	#Yrs	(%)	#Yrs	(%)
Extremely wet	above 2	5	4	5	4	4	3	8	7	5	4
Very wet	1.5 to 2	4	3	7	6	7	6	3	3	6	5
Wet	1.0 to 1.5	8	7	5	4	9	8	7	6	7	6
Normal	-1.0 to 1.0	86	72	84	70	81	68	82	68	86	72
Dry	-1 to -1.5	15	13	18	15	16	13	16	13	16	13
Very dry	-1.5 to -2	2	2	1	1	3	3	4	3	0	0
Extremely dry	below -2	0	0	0	0	0	0	0	0	0	0
Excess	> Normal	17	14	17	14	20	17	18	15	18	15
Deficit	< Normal	17	14	19	16	19	16	20	17	16	13
	SPI	MAM-1		MAM-2		MAM-3		MAM-4		MAM-5	
Extremely wet	above 2	5	4	4	3	5	4	4	3	6	5
Very wet	1.5 to 2	4	3	6	5	5	4	6	5	3	3
Wet	1.0 to 1.5	10	8	9	8	10	8	6	5	5	4
Normal	-1.0 to 1.0	85	71	80	67	87	73	84	70	86	72
Dry	-1 to -1.5	10	8	13	11	7	6	12	10	14	12
Very dry	-1.5 to -2	4	3	8	7	4	3	6	5	6	5
Extremely dry	below -2	2	2	0	0	2	2	2	2	0	0
Excess	> Normal	19	16	19	16	20	17	16	13	14	12
Deficit	< Normal	16	13	21	18	13	11	20	17	20	17
	SPI	JJA-1		JJA-2		JJA-3		JJA-4		JJA-5	
Extremely wet	above 2	5	4	6	5	5	4	4	3	5	4
Very wet	1.5 to 2	3	3	2	2	6	5	5	4	3	3
Wet	1.0 to 1.5	8	7	7	6	5	4	7	6	8	7
Normal	-1.0 to 1.0	88	73	89	74	86	72	88	73	85	71
Dry	-1 to -1.5	10	8	10	8	14	12	8	7	14	12
Very dry	-1.5 to -2	2	2	2	2	2	2	7	6	2	2
Extremely dry	below -2	4	3	4	3	2	2	1	1	3	3
Excess	> Normal	16	13	15	13	16	13	16	13	16	13
Deficit	< Normal	16	13	16	13	18	15	16	13	19	16
	SPI	SON-1		SON-2		SON-3		SON-4		SON-5	
Extremely wet	above 2	3	3	5	4	4	3	6	5	4	3
Very wet	1.5 to 2	5	4	6	5	2	2	2	2	10	8
Wet	1.0 to 1.5	6	5	9	8	8	7	5	4	7	6
Normal	-1.0 to 1.0	84	70	89	74	89	74	92	77	80	67
Dry	-1 to -1.5	13	11	5	4	8	7	12	10	17	14
Very dry	-1.5 to -2	8	7	6	5	8	7	3	3	2	2
Extremely dry	below -2	1	1	0	0	1	1	0	0	0	0
Excess	> Normal	14	12	20	17	14	12	13	11	21	18
Deficit	< Normal	22	18	11	9	17	14	15	13	19	16

DJF, December-January-February; MAM, March-April-May; JJA, Jun-July-August; SON, September-October-November

to increase throughout the 21st century (Houghton et al. 1990; WMO 2020). This increase in global temperature is associated with greater increases of daily Tmin than Tmax (Easterling et al. 1997). Overall, the significant increase of annual temperature in Ethiopia from 1901

to 2020 can be attributed to an increase in the annual Tmin (the rate of increase has been greater for Tmin than Tmax). This increase in temperature leads to an increase in water loss and will cause more severe droughts in much of Ethiopia in the future.

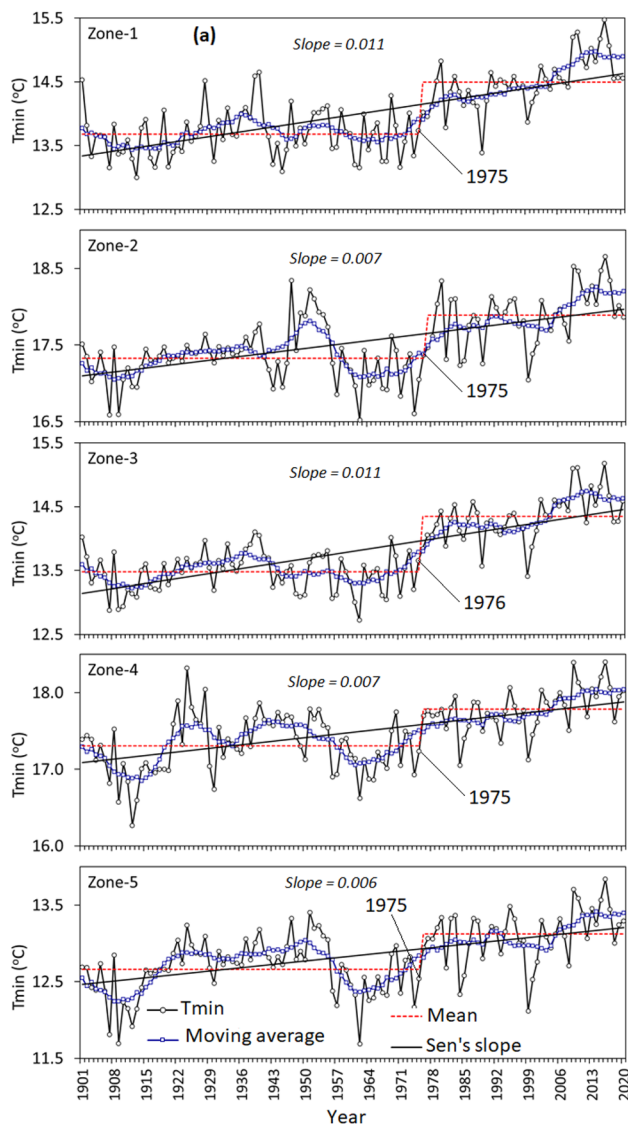


Fig. 12 Trends and changes in (a) minimum temperature (T_{min} ; °C); (b) maximum temperature (T_{max} ; °C); (c) mean temperature (T_{mean} ; °C) in five climate zones from 1901 to 2020. The dotted lines indicate the Pettitt test homogeneity trend result at a significance level $\alpha = 0.05$ and show the mean value of annual rainfall. The black solid lines indicate the Sen's slope for the trend

3.3.2 Inter-seasonal spatial and temporal variability and trend of temperature

The seasonal T_{min} ranged from approximately 2°C to 23°C, 5°C to 25°C, 5°C to 28°C, and 4°C to 25°C, respectively, during the winter (DJF), spring (MAM), summer (JJA) and autumn (SON) seasons (Fig. 13a). The average T_{min} was relatively high in Zone-2 (range: 15°C±4°C in DJF to 21°C±5°C in JJA) and Zone-4 (range: 16°C±3°C in DJF to 19°C±4°C in MAM) in all seasons. This higher average T_{min} was associated with the amounts of rainfall in each

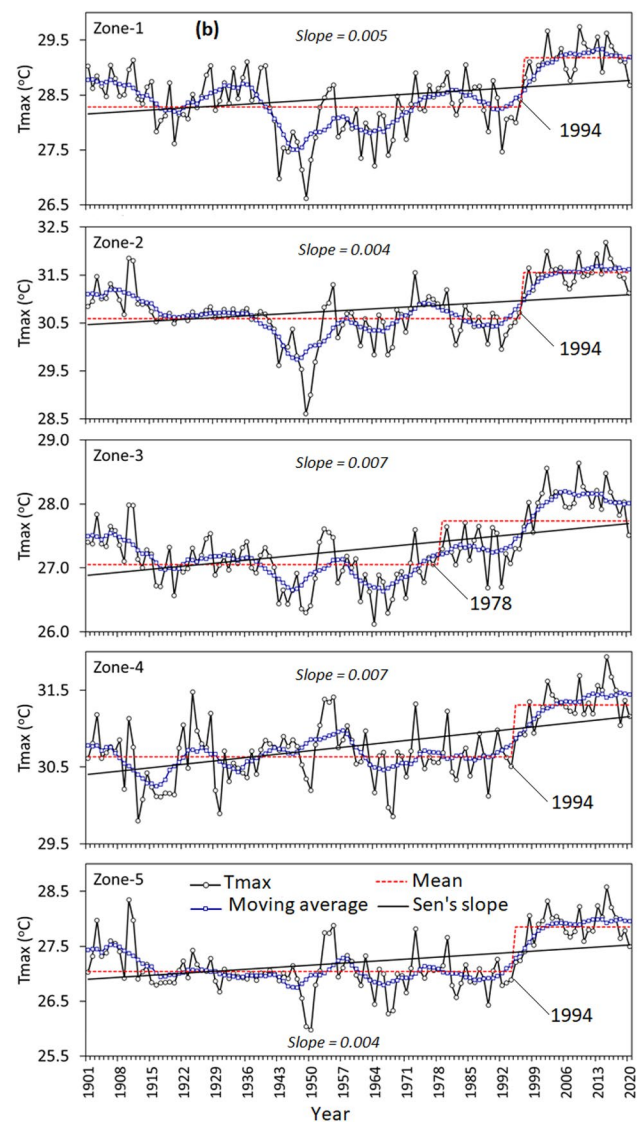


Fig. 12 (continued)

zone. Zone-2 and Zone-4 received high amounts of rainfall in the summer and spring, respectively (Fig. 6). In contrast, the average T_{min} was lower in Zone-5 (range: 10°C±3°C in DJF to 14°C±4°C in MAM) during all seasons except the summer (Fig. 13a). As shown in Fig. 13b, the seasonal T_{max} ranged from ~16°C to 39°C, in the autumn (SON) and summer (JJA) season, respectively. The country's average T_{max} (27°C±4°C) was very similar during winter, summer, and autumn, but the average T_{max} increased by 2°C during the spring. The T_{max} was relatively high in Zone-2 (32°C±5°C in JJA) and Zone-4 (range: 30°C±3°C in DJF and SON to 31°C±3°C in MAM) during the study period. The T_{max} was relatively low in Zone-3 (24°C±3°C in JJA and 25°C±3°C in SON) and Zone-5 (26°C±3°C in DJF and 27°C±4°C (MAM)). The T_{mean} was a minimum (10°C) and a maximum (34°C) during the autumn and summer, respectively

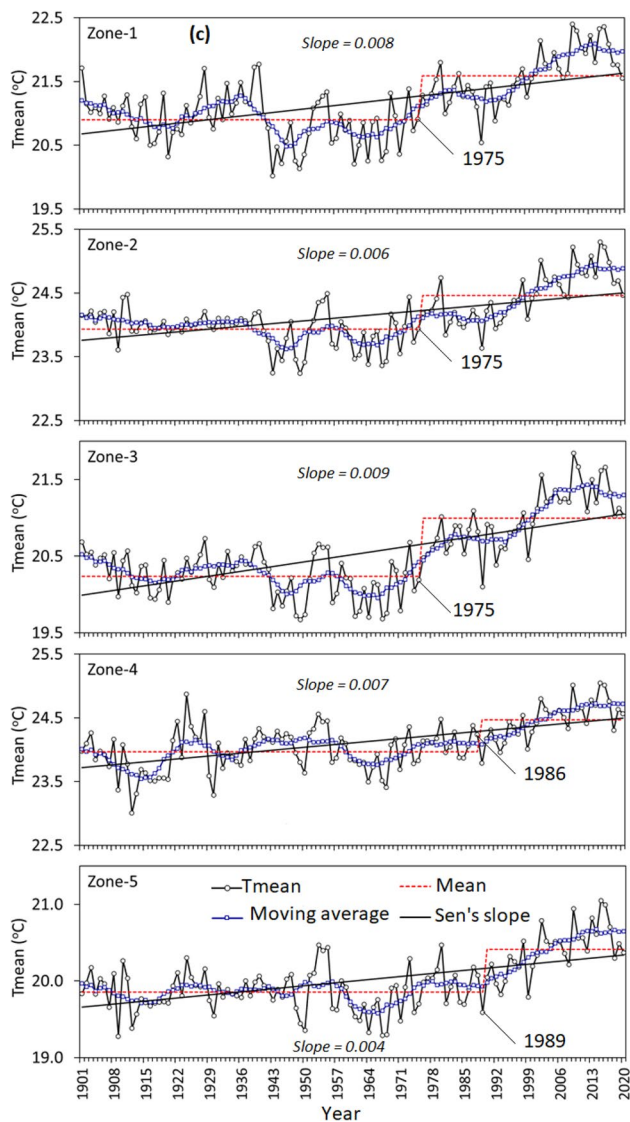


Fig. 12 (continued)

(Fig. 13c). The Tmean was higher in Zone-2 and Zone-4 from 1901 to 2020; the upper limit of Tmean was $27^{\circ}\text{C} \pm 5^{\circ}\text{C}$ in JJA, and the lower limit was $22^{\circ}\text{C} \pm 5^{\circ}\text{C}$ in DJF, respectively (Table TS6). In general, spring (MAM) was the hottest season in Ethiopia in all rainfall zones from 1901 to 2020.

The CV of Tmin, Tmax, and Tmean varied from approximately 2% to 26%, 6% to 19%, and 1% to 5%, respectively (Fig. 13). The indication was that the seasonal variation was low for Tmean compared with Tmin and Tmax. Low temperatures (Tmin, Tmax, and Tmean) were correlated with higher CV values and vice versa. For instance, inter-seasonal variations of temperature (Tmin, Tmean, and Tmax) were low in the northeast, southeast, and eastern parts of Ethiopia (Zone-2, Zone-4, and small parts of Zone-5) in all seasons. In contrast, there were high inter-seasonal variations of seasonal temperature (Tmin, Tmean, and Tmax) in the

northwest, southwest, and western (all of Zone-1 and Zone-3, and parts of Zone-5 and Zone-4) parts of Ethiopia in all seasons (Fig. 13). During the winter (DJF), the intraseasonal variations of temperature (especially Tmin and Tmax) were greater. This result was confirmed by the long-term seasonal anomalies of Tmin, Tmax, and Tmean (Fig. FS6–FS8).

The spatial distribution (Fig. 13) and temporal trends (Fig. 14) of seasonal temperature (Tmin, Tmax, and Tmean) showed a significant (at $\alpha = 0.05$) increasing trend in all rainfall zones. The spatial increase in the seasonal Tmin varied by less than 1°C (more than three zones) and by 3°C (only Zone-1 in the spring) over 120 years (Table TS6). Similarly, seasonal Tmax significantly increased by approximately 1°C (Zone-4 in DJF; Zone -2, Zone-4, and Zone-5 in JJA; and Zone-4 and Zone-5 in SON) to 2°C (except Zone-1 in DJF; all zones in MAM; Zone-1 and Zone-3 in JJA; Zone-1 to Zone-3 in SON) over 120 years (Table TS6). Interestingly, there was a significant increase in seasonal Tmean across all rainfall zones of approximately 1°C during all seasons over 120 years (Table TS6).

There was a statistically significant monotonic and non-homogeneous temporal trend in seasonal temperature (Tmin, Tmax, and Tmean) in all rainfall zones over the study period (Fig. 14 and Tables TS7–TS9). This trend was confirmed by the changes in seasonal temperature from 1901 to 2020. We thus rejected the null hypotheses for the MK and Pettitt's tests for seasonal Tmin, Tmax, and Tmean trends in all rainfall zones (Tables TS7–TS9). The seasonal Tmin, Tmax, and Tmean increased significantly by 0.48°C (SON) to 1.92°C (MAM), 0.36°C (DJF and JJA) to 1.08°C (MAM), and 0.6°C (SON and JJA) to 1.44°C (MAM), respectively, from 1901 to 2020 (Fig. 14). In general, large and small increases of Tmin were observed in spring and autumn, respectively, across rainfall zones. Compared to other rainfall zones, a greater increase of the seasonal Tmin was apparent in Zone-1 (in DJF, MAM, and SON) and Zone-3 (in all seasons) (Fig. 14). The increase of the seasonal Tmax was also greater in Zone-4 (in DJF and JJA) and Zone-3 (in MAM and SON). Likewise, a greater increase of Tmean was apparent in Zone-3 (in all seasons), Zone-1 (MAM), and Zone-5 (JJA) than in other rainfall zones (Fig. 14). In all rainfall zones, the homogeneity test results indicated that the inflection point for seasonal Tmin was in the 1970s in all seasons except the winter in Zone-2 (the 1930s) and in Zone-4 and Zone-5 (the 1920s) (Fig. 14a). For seasonal Tmax, the inflection point was in the 1970s in JJA (for all zones) and SON (for Zone-1 and Zone-3) and the 1990s in DJF and MAM (for all zones) and SON (for only Zone-2 and Zone-5) (Fig. 14b). Similarly, seasonal Tmean has an inflection point in the 1970s and 1990s. The indication was that the inflection point of Tmean was strongly influenced by Tmin and Tmax (Fig. 14c). After the inflection points, positive

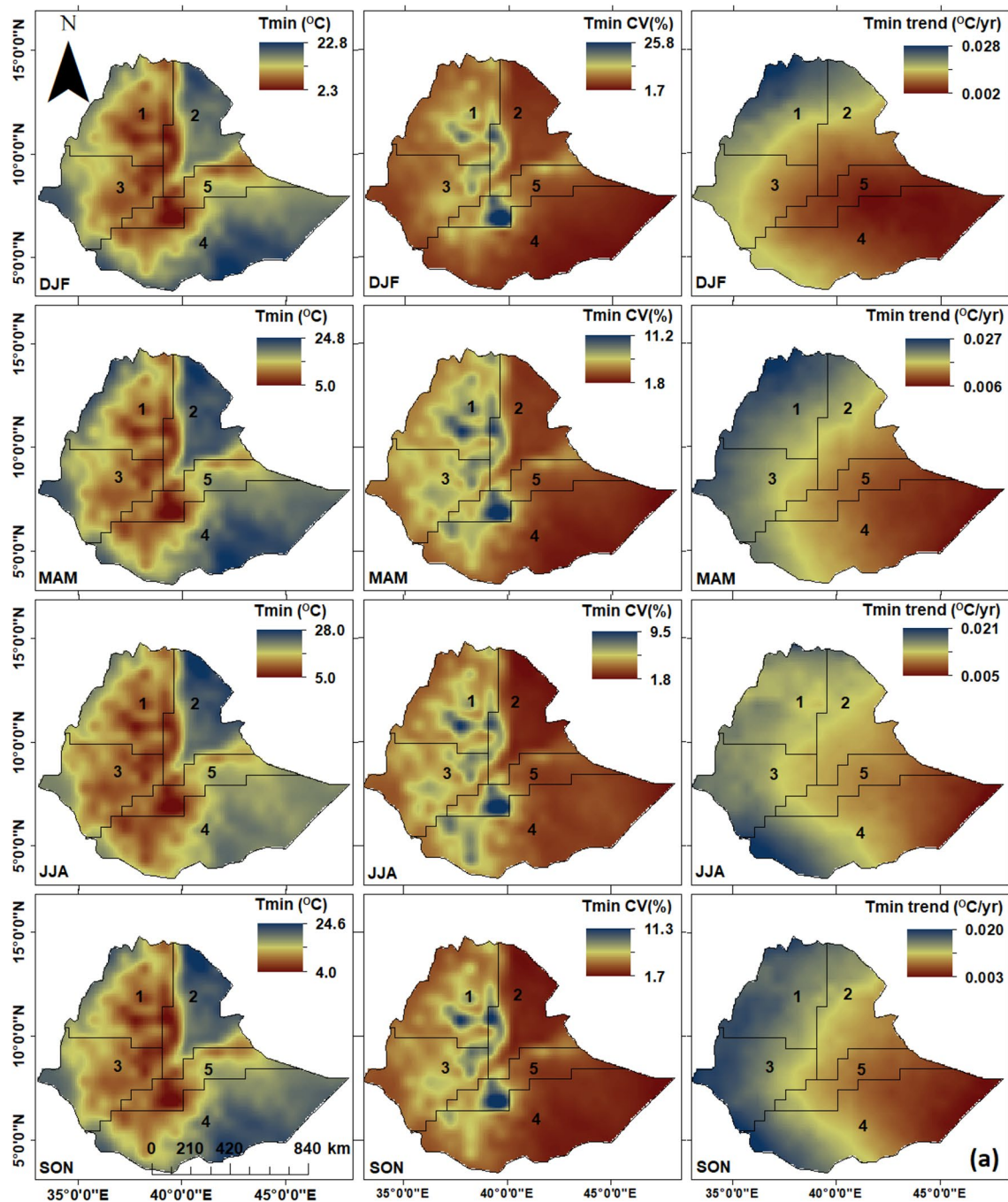


Fig. 13 Spatial distribution of seasonal (a) minimum temperature (Tmin; °C); (b) maximum temperature (Tmax; °C); (c) mean temperature (Tmean; °C) during the period 1901–2020: mean value (left side), coefficient of variation (CV, middle), and trend (rate of change

in °C per year; right side). In all areas, the trend is statistically significant at $\alpha = 0.05$. DJF, December–January–February; MAM, March–April–May; JJA, Jun–July–August; SON, September–October–November

seasonal temperature anomalies (Tmin, Tmax, and Tmean) were more frequently apparent than before the inflection points (more negative anomalies were observed) (Figs. FS6–FS8).

The monthly temporal trend analysis also revealed a statistically significant trend in monthly Tmin in all

rainfall zones except Zone-5 in the months of January and October (Table TS7). No significant monotonic and non-homogeneous trend in monthly Tmax was detected in the months of January (Zone-1, Zone -2, and Zone-3), February (Zone-1), March (Zone-2 and Zone-5), June (except Zone-4), and December (Zone-1 and Zone-3) from 1901

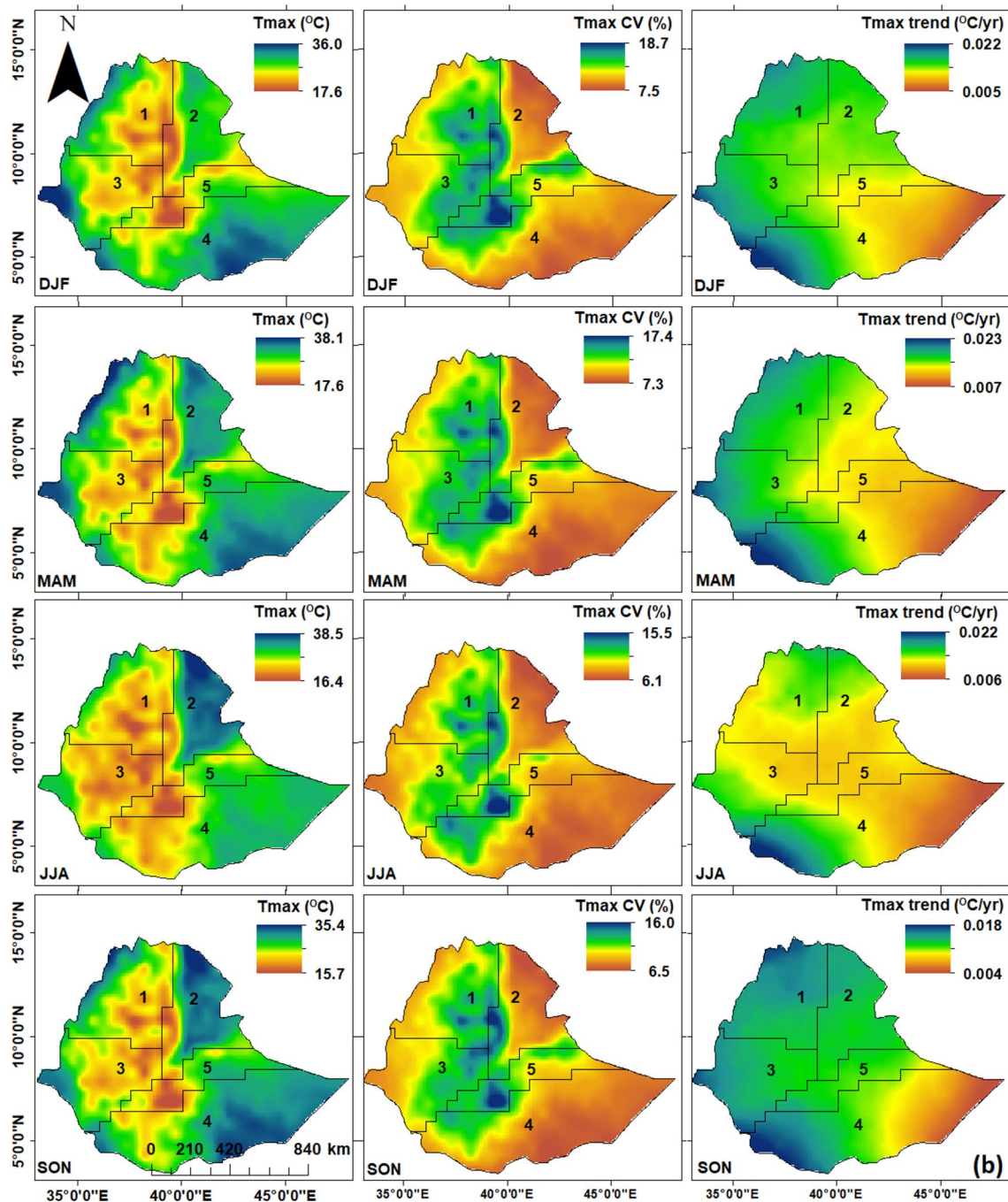


Fig. 13 (continued)

to 2020 (Table TS8). Unlike some monthly Tmax values, a significant increasing trend of monthly Tmean was observed from 1901 to 2020 in all rainfall zones except for the month of June in Zone-1 (Table TS9).

Overall, the spring (MAM) and winter (DJF) seasons are considered the hottest and coldest seasons, respectively, in Ethiopia in all rainfall zones. Similar findings have been reported in previous studies in the upper Blue

Nile basin (part of Zone-1 and Zone-3, Conway et al., 2000) and Lake Hayk basin (on the border of Zone-1 and Zone-2, Mewded et al. 2022). Rainfall, cloudy conditions, and energy used for evapotranspiration reduce peak temperatures in summer (JJA). High inter-seasonal variability of seasonal temperature (Tmin, Tmax, and Tmean) was observed in winter (DJF) during the study period (Fig. 14). Likewise, the inter-seasonal variability

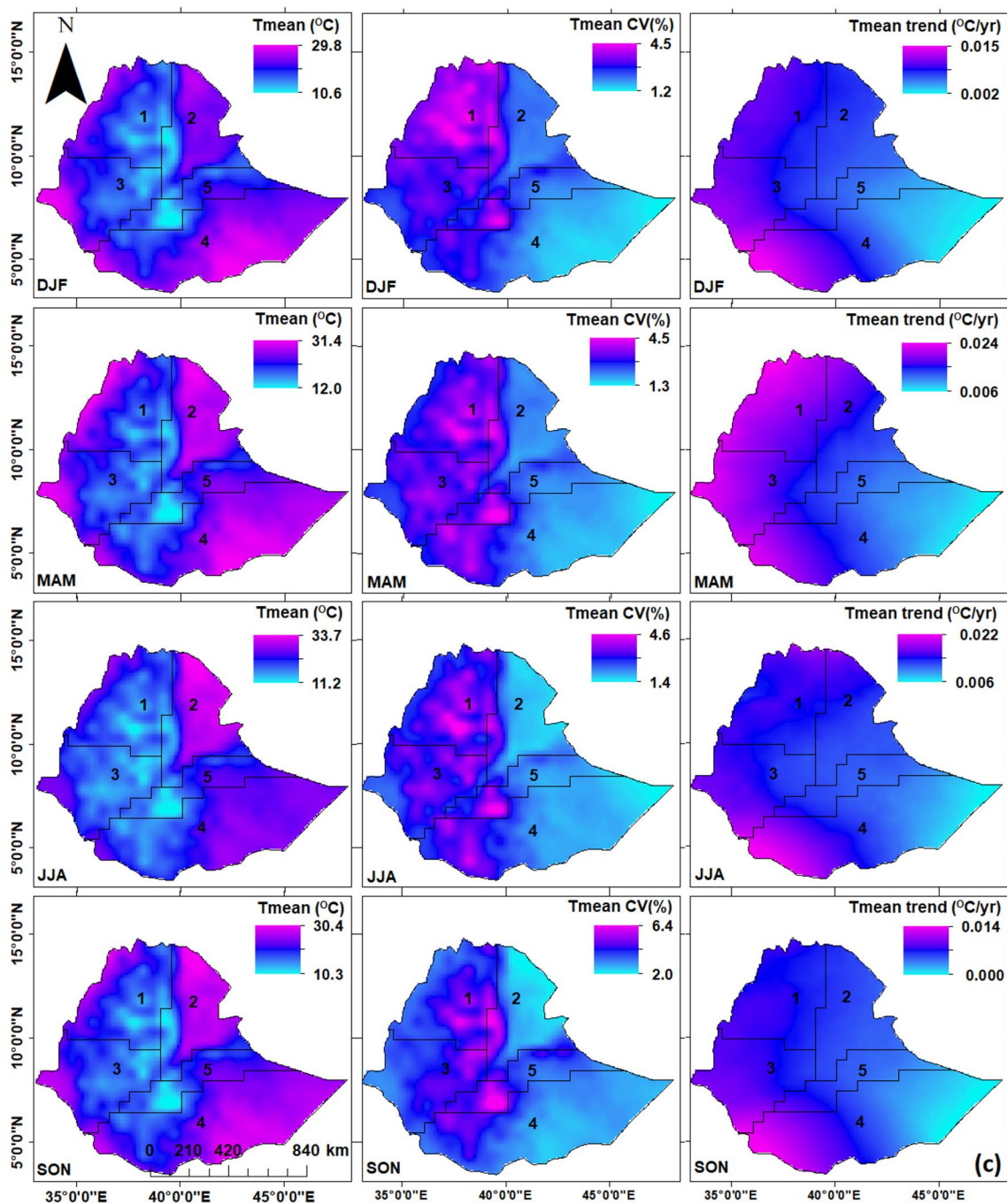


Fig. 13 (continued)

was greater for T_{max} than T_{min} and T_{mean} in all rainfall zones (Fig. 14a). However, the seasonal T_{min} increased at a higher rate than the seasonal T_{max} and T_{mean} from 1901 to 2020 in all rainfall zones. A number of previous studies in Ethiopia have reported similar results in the upper Blue Nile basin (Zone-1 and some parts of Zone-3, Conway 2000; Mengistu et al. 2014), central Ethiopia (Zone-5, Conway et al. 2004), western Ethiopia (Bekuma

et al. 2022), southern Ethiopia (Zone-4, Belay et al. 2021), southwestern Ethiopia (part of Zone-3 and Zone-4, Habte et al. 2021), and eastern Ethiopia (Zone-2 and Zone-5, Bayable et al. 2021). The rate of change, however, varied as a function of the source of data, the length of the study period, and the size of the area studied. Our finding of increasing trends in the seasonal T_{min} and T_{max} in all seasons contradicted the results (non-significant

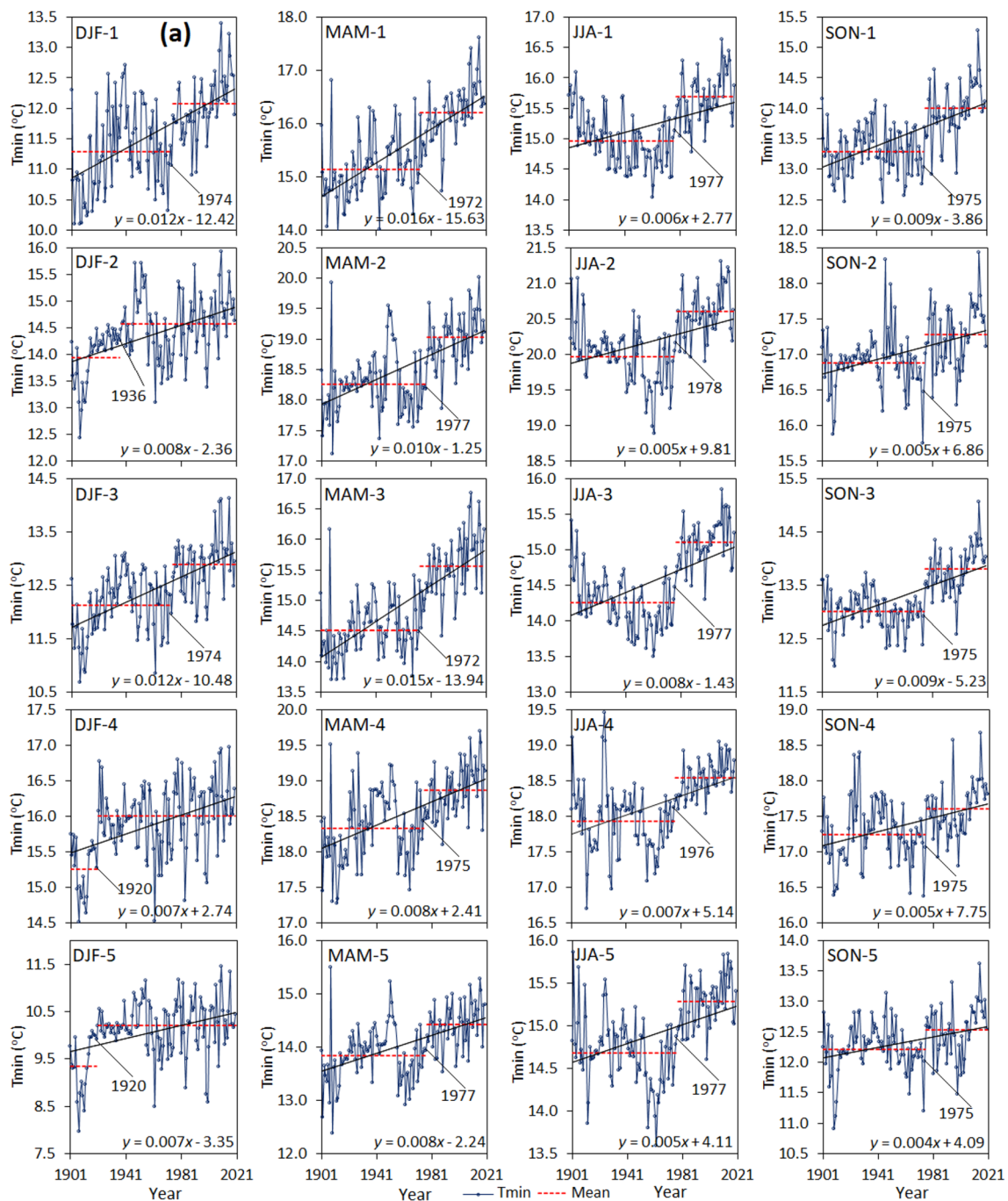


Fig. 14 Trends and changes in seasonal (a) minimum Temperature (T_{min} ; °C); (b) maximum temperature (T_{max} ; °C); (c) average temperature (T_{mean} ; °C) in five climate zones of Ethiopia from 1901 to 2020. The dashed lines indicate the Pettitt test homogeneity trend

decreasing trends in seasonal T_{min} and T_{max}) reported by Alemayehu et al. (2020) in western Ethiopia from 1983 to 2016. In contrast to our findings, a non-significant increasing trend in T_{max} has been reported during MAM in northern parts of Ethiopia, and a significant decreasing trend has been detected in western (MAM) and

eastern (JJA and SON) parts of Ethiopia (Gebrechorkos et al. 2019). The difference may be attributed to the data sources and the length of the study period. For example, Gebrechorkos et al. (2019) used Observational-Reanalysis Hybrid data for temperature from 1979 to 2010. Zonal level comparison results also revealed high inter-seasonal

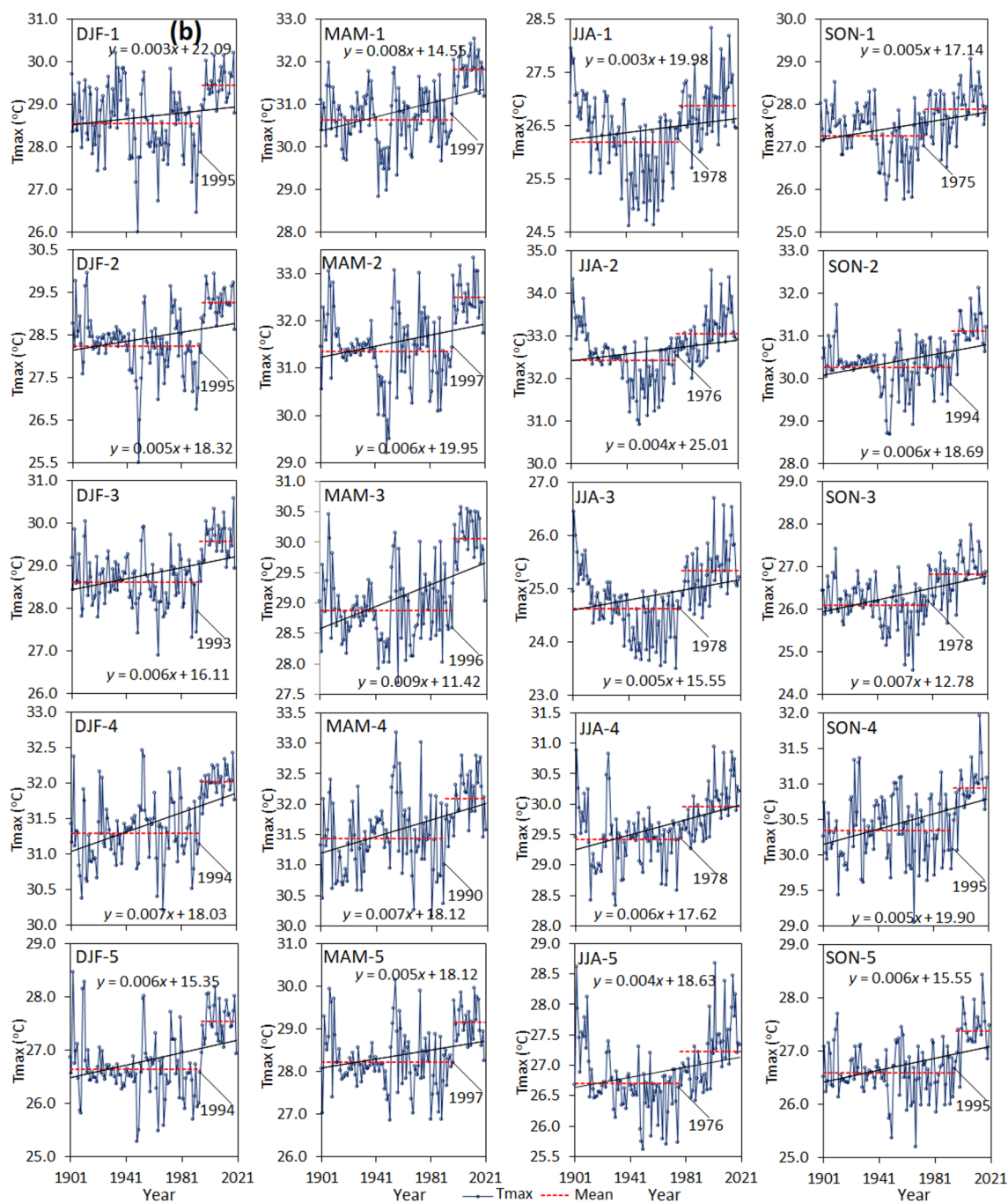


Fig. 14 (continued)

variability of temperature (T_{min} , T_{max} , and T_{mean}) in Zone-1, Zone-3, and Zone-5. Like our results, significant increasing trends of monthly T_{min} and non-significant increasing trends of monthly T_{max} (in some months) have been reported in some areas of Ethiopia (e.g., Alemayehu et al. 2020; Asfaw et al. 2018; Bekuma et al. 2022). Rising seasonal temperatures have direct and indirect impacts

on food security and the livelihood of people, including increases in human and livestock diseases, reductions in seasonal crop productivity, and increases in water scarcity, particularly in tropical climates (e.g., Abeje et al. 2019; WMO 2020). Decision-makers should therefore consider in advance all possible measures to mitigate future impacts on the region.

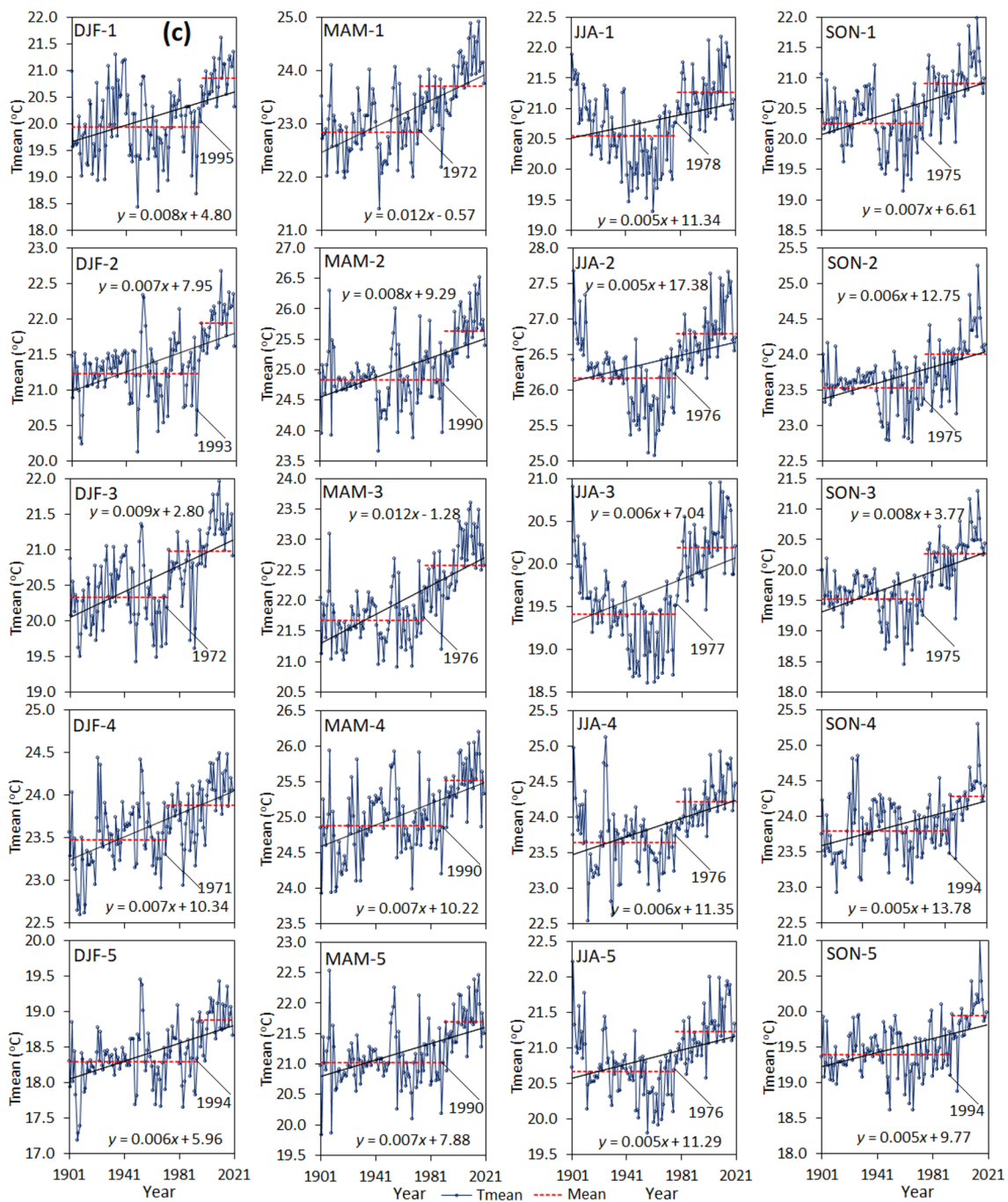


Fig. 14 (continued)

4 Conclusions

In Ethiopia, a region characterized by frequent droughts and long-term climate variability, trend analysis is extremely important for anticipating and minimizing possible threats. In this study, we examined the spatiotemporal variability and trends of Ethiopian climate (rainfall and temperature) from

1901 to 2020 using monthly Climatic Research Unit (CRU 4.05) gridded dataset by integrating observed rainfall and temperature data. Five different homogeneous rainfall zones were identified using long-term monthly peaks, seasonal rainfall patterns, and pixel-based monthly rainfall correlation coefficient techniques. The results revealed that there was high spatiotemporal variability of rainfall and temperature

on annual and seasonal timescales in all rainfall zones. However, for both climate parameters, the inter-seasonal variability was more pronounced than the interannual variability in all rainfall zones. The trends of annual rainfall revealed that there were non-significant decreases of as much as -1.39 mm per year and increases of as much as $+1.22$ mm per year over approximately 27% and 48% of the country from 1901 to 2020, respectively. However, statistically significant ($\alpha = 0.05$) trends in rainfall were observed in some areas (22%) of the country at annual and seasonal timescales, whereas no significant temporal trends of rainfall were observed in all seasons (except summer in Zone-3) and rainfall zones. The long-term PCI spatial analysis results also revealed that the country exhibited moderate to strongly regular annual and seasonal rainfall patterns, except during the summer (when the rainfall distribution was uniform). The indication was that rainfall was highly seasonal throughout the course of the year. The annual and seasonal SPI values characterized years and seasons as wet (positive anomalies) and dry (negative anomalies) in Ethiopia. There was a higher percentage of negative anomalies than positive anomalies during the study period. The 1984 deficit and 1967 excess rainy years were observed in all rainfall zones of Ethiopia.

Unlike rainfall, there was a spatial and temporal statistically significant ($\alpha = 0.05$) increasing trend in annual and seasonal temperature in all rainfall zones of the country. The spatial and temporal increasing trend rate of mean temperature (T_{mean}) at annual and seasonal timescale ranged from 0.24°C to 1.92°C and 0.72°C to 1.08°C , respectively, from 1901 to 2020. In all rainfall zones, T_{min} increased at a faster rate than T_{max} and T_{mean} over the study period, and the change in T_{mean} was highly influenced by T_{min} . Increasing temperatures are expected to increase evapotranspiration, increase water losses by evaporation, and cause more severe droughts across large parts of the country. Areas severely affected by drought or deficit rainfall thus require particular attention and further study to reduce possible negative impacts. This study will contribute to a better understanding of the past climate of Ethiopia in different rainfall zones for future climate projection and can be used in planning for adaptation measures and mitigation of impacts of changing climate and climate extremes. The classification of rainfall zones should also facilitate estimates of design rainfall for hydraulic structures and the arrangement of cropping schedules.

Supplementary Information The online version contains supplementary material available at <https://doi.org/10.1007/s00704-023-04572-4>.

Acknowledgment We thank the Ethiopian National Meteorological Services Agency and the Arid Land Research Centre, Tottori University, for providing meteorological data and an appropriate research environment, respectively.

Authors' contributions **Mulatu Liyew Berihun:** Conceptualization, Methodology, Software, Formal analysis, Investigation, Resources,

Data curation, Writing-original draft, Writing-review & editing, Visualization. **Atsushi Tsunekawa, Nigussie Haregeweyn, and Mitsuru Tsubo:** Resources, Writing -review & editing, Visualization, Supervision, Project administration, Funding acquisition. **Hiroshi Yasuda:** Methodology; Writing-review & editing, Visualization. **Ayele Almaw Fenta and Yihun Taddele Dile, Haimanote Kebede Bayabil and Seifu Admassu Tilahun:** Writing-review & editing, Visualization.

Funding This research was funded by the Science and Technology Research Partnership for Sustainable Development (SATREPS, grant number JPMJSA1601), Japan Science and Technology Agency (JST) / Japan International Cooperation Agency (JICA).

Data availability The datasets used and/or analyzed during the current study are available from the corresponding author on reasonable request

Declarations

Ethics approval and consent to participate Not applicable

Consent for publication Not applicable

Competing interests The authors have not disclosed any competing interests.

Open Access This article is licensed under a Creative Commons Attribution 4.0 International License, which permits use, sharing, adaptation, distribution and reproduction in any medium or format, as long as you give appropriate credit to the original author(s) and the source, provide a link to the Creative Commons licence, and indicate if changes were made. The images or other third party material in this article are included in the article's Creative Commons licence, unless indicated otherwise in a credit line to the material. If material is not included in the article's Creative Commons licence and your intended use is not permitted by statutory regulation or exceeds the permitted use, you will need to obtain permission directly from the copyright holder. To view a copy of this licence, visit <http://creativecommons.org/licenses/by/4.0/>.

References

- Abebe BA, Grum B, Degu AM, Goitom H (2022) Spatio-temporal rainfall variability and trend analysis in the Tekeze-Atbara River basin, northwestern Ethiopia. *Meteorol Appl* 29(2):e2059
- Abeje MT, Tsunekawa A, Haregeweyn N, Nigussie Z, Adgo E, Ayalew Z, Tsubo M, Elias A, Berihun D, Quandt A, Berihun ML (2019) Communities' livelihood vulnerability to climate variability in Ethiopia. *Sustainability* 11(22):6302
- Ahmed K, Shahid S, Wang X, Nawaz N, Khan N (2019) Evaluation of gridded precipitation datasets over arid regions of Pakistan. *Water* 11(2):210
- Alemayehu A, Maru M, Bewket W, Assen M (2020) Spatiotemporal variability and trends in rainfall and temperature in Alwero watershed, western Ethiopia. *Environ Syst Res* 9(1):1–15
- Alemu MM, Bawoke GT (2020) Analysis of spatial variability and temporal trends of rainfall in Amhara region, Ethiopia. *J Water Clim Change* 11(4):1505–1520
- Alhamsry A, Fenta AA, Yasuda H, Kimura R, Shimizu K (2019) Seasonal rainfall variability in Ethiopia and its long-term link to global sea surface temperatures. *Water* 12(1):55
- Asfaw A, Simane B, Hassen A, Bantider A (2018) Variability and time series trend analysis of rainfall and temperature in northcentral

- Ethiopia: A case study in Woleka sub-basin. *Weather Clim Extrem* 19:29–41
- Ayugi BO, Wen W, Chepkemio D (2016) Analysis of spatial and temporal patterns of rainfall variations over Kenya. *J Environ Earth Sci* 6(11)
- Bayable G, Amare G, Alemu G, Gashaw T (2021) Spatiotemporal variability and trends of rainfall and its association with Pacific Ocean Sea surface temperature in West Harege Zone, Eastern Ethiopia. *Environ Syst Res* 10(1):1–21
- Bekuma, T., Mamo, G. and Regassa, A., 2022 Variability and trends of climate in east Wollega zone, Western Ethiopia. In *IOP Conference Series: Earth and Environmental Science* (1016, 1, 012032 IOP Publishing.
- Belay A, Demissie T, Recha JW, Oludhe C, Osano PM, Olaka LA, Solomon D, Berhane Z (2021) Analysis of climate variability and trends in Southern Ethiopia. *Climate* 9(6):96
- Berhanu B, Seleshi Y, Melesse AM (2014) Surface water and groundwater resources of Ethiopia: potentials and challenges of water resources development. In: *Nile River Basin*. Springer Link, pp 97–117. https://doi.org/10.1007/978-3-319-02720-3_6
- Berihun ML, Tsunekawa A, Haregeweyn N, Meshesha DT, Adgo E, Tsubo M, Masunaga T, Fenta AA, Sultan D, Yibeltal M, Ebabu K (2019) Hydrological responses to land use/land cover change and climate variability in contrasting agro-ecological environments of the Upper Blue Nile basin, Ethiopia. *Sci Total Environ* 689:347–365
- Berihun ML, Tsunekawa A, Haregeweyn N, Dile YT, Tsubo M, Fenta AA, Meshesha DT, Ebabu K, Sultan D, Srinivasan R (2020) Evaluating runoff and sediment responses to soil and water conservation practices by employing alternative modeling approaches. *Sci Total Environ* 747:141118
- Broman D, Rajagopalan B, Hopson T, Gebremichael M (2020) Spatial and temporal variability of East African Kiremt season precipitation and large-scale teleconnections. *Int J Climatol* 40(2):1241–1254
- Burn DH (1994) Hydrologic effects of climatic change in west-central Canada. *J Hydrol* 160(1-4):53–70
- Central Statistical Agency (CSA) (2018) Ethiopia National Child Labour Survey 2015. Addis Ababa, International Labour Organization (ILO), p 172
- Cheung WH, Senay GB, Singh A (2008) Trends and spatial distribution of annual and seasonal rainfall in Ethiopia. *Int J Climatol* 28(13):1723–1734
- Conway D (2000) The climate and hydrology of the Upper Blue Nile River. *Geogr J* 166(1):49–62
- Conway D, Mould C, Bewket W (2004) Over one century of rainfall and temperature observations in Addis Ababa, Ethiopia. *Int J Climatol* 24(1):77–91
- Conway D, Schipper ELF (2011) Adaptation to climate change in Africa: Challenges and opportunities identified from Ethiopia. *Glob Environ Chang* 21(1):227–237
- Dai A, Trenberth KE, Karl TR (1998) Global variations in droughts and wet spells: 1900–1995. *Geophys Res Lett* 25(17):3367–3370
- Desanker PV (2002) The Impact of Climate Change of Life in Africa: Climate Change and Vulnerability in Africa. WorldWide Fund for Nature, Washington DC, USA
- Degefu MA, Rowell DP, Bewket W (2017) Teleconnections between Ethiopian rainfall variability and global SSTs: observations and methods for model evaluation. *Meteorol Atmos Phys* 129(2):173–186
- Dinku T, Connor SJ, Ceccato P et al (2008) Comparison of global gridded precipitation products over a mountainous region of Africa. *Int J Climatol* 28:1627–1638. <https://doi.org/10.1002/joc.1669>
- Diro GT, Grimes DIF, Black E (2011) Teleconnections between Ethiopian summer rainfall and sea surface temperature: part II. *Season Forecast Clim Dynamics* 37(1):121–131
- Enfield DB, Mestas-Nuñez AM, Trimble PJ (2001) The Atlantic multi-decadal oscillation and its relation to rainfall and river flows in the continental US. *Geophys Res Lett* 28(10):2077–2080
- Easterling DR, Evans JL, Groisman PY, Karl TR, Kunkel KE, Ambenje P (2000) Observed variability and trends in extreme climate events: a brief review. *Bull Am Meteorol Soc* 81(3):417–426
- Easterling DR, Horton B, Jones PD, Peterson TC, Karl TR, Parker DE, Salinger MJ, Razuvayev V, Plummer N, Jamason P, Folland CK (1997) Maximum and minimum temperature trends for the globe. *Science* 277(5324):364–367
- Ethiopia Road Authorities (ERA) (2013) Drainage Design Manual. Federal Democratic Republic of Ethiopia Ethiopian Roads Administration, Addis Ababa
- Fazzini M, Bisci C, Billi P (2015) The climate of Ethiopia. In: *Landscapes and landforms of Ethiopia*. Springer, Dordrecht, pp 65–87
- Fenta AA, Tsunekawa A, Haregeweyn N, Tsubo M, Yasuda H, Kawai T, Ebabu K, Berihun ML, Belay AS, Sultan D (2021) Agroecology-based soil erosion assessment for better conservation planning in Ethiopian river basins. *Environ Res* 195:110786
- Fenta AA, Yasuda H, Shimizu K, Haregeweyn N, Kawai T, Sultan D, Ebabu K, Belay AS (2017) Spatial distribution and temporal trends of rainfall and erosivity in the Eastern Africa region. *Hydrol Process* 31(25):4555–4567
- Funk C, Peterson P, Landsfeld M, Pedreros D, Verdin J, Shukla S, Husak G, Rowland J, Harrison L, Hoell A, Michaelsen J (2015) The climate hazards infrared precipitation with stations—a new environmental record for monitoring extremes. *Sci Data* 2(1):1–21
- Gebrechorkos SH, Hülsmann S, Bernhofer C (2019) Long-term trends in rainfall and temperature using high-resolution climate datasets in East Africa. *Sci Rep* 9(1):1–9
- Gleixner S, Keenlyside N, Viste E, Korecha D (2017) The El Niño effect on Ethiopian summer rainfall. *Clim Dyn* 49(5):1865–1883
- Gurara MA, Tolche AD, Jilo NB, Kassa AK (2022) Annual and seasonal rainfall trend analysis using gridded dataset in the Wabe Shebele River Basin, Ethiopia. *Theor Appl Climatol* 150(1-2):263–281
- Habte A, Mamo G, Worku W, Ayalew D, Gayler S (2021) Spatial variability and temporal trends of climate change in Southwest Ethiopia: association with farmers' perception and their adaptation strategies. *Adv Meteorol* 2021
- Harris I, Osborn TJ, Jones P, Lister D (2020) Version 4 of the CRU TS monthly high-resolution gridded multivariate climate dataset. *Sci Data* 7(1):1–18
- Houghton JT, Jenkins GJ, Ephraums JJ (1990) Climate change: the IPCC scientific assessment. *Am Sci* 80(6)
- Hurni H (1988) Degradation and conservation of the resources in the Ethiopian highlands. *Mt Res Dev*:123–130
- Intergovernmental Panel on Climate Change (IPCC) (2007) Climate change 2007: synthesis report. IPCC
- Intergovernmental Panel on Climate Change (IPCC) (2019) Climate Change and Land: an IPCC special report on climate change, desertification, land degradation, sustainable land management, food security, and greenhouse gas fluxes in terrestrial ecosystems. IPCC
- Intergovernmental Panel on Climate Change (IPCC) (2014) Climate Change 2014: Impacts, Adaptation, and Vulnerability; Part a: Global and Sectoral Aspects. In: *Contribution of Working Group II to the Fifth Assessment Report of the Intergovernmental Panel on Climate Change*. Cambridge University Press, Cambridge, United Kingdom and New York, NY, USA, p 1132
- Jury MR, Funk C (2013) Climatic trends over Ethiopia: regional signals and drivers. *Int J Climatol* 33(8):1924–1935

- Korecha D, Barnston AG (2007) Predictability of June–September rainfall in Ethiopia. *Mon Weather Rev* 135(2):628–650
- Mengistu D, Bewket W, Lal R (2014) Recent spatiotemporal temperature and rainfall variability and trends over the Upper Blue Nile River Basin, Ethiopia. *Int J Climatol* 34(7):2278–2292
- Mewded M, Abebe A, Tilahun S, Agide Z (2022) Climate variability and trends in the Endorheic Lake Hayk basin: implications for Lake Hayk water level changes in the lake basin, Ethiopia. *Environ Syst Res* 11(1):1–17
- McKee TB, Doesken NJ, Kleist J (1993) The relationship of drought frequency and duration to time scales. *Proc 8th Conf Appl Climatol* 17(22):179–183
- Moreno J, Møller AP (2011) Extreme climatic events in relation to global change and their impact on life histories. *Current Zool* 57(3):375–389
- Mulugeta S, Fedler C, Ayana M (2019) Analysis of long-term trends of annual and seasonal rainfall in the Awash River basin, Ethiopia. *Water* 11(7):1498
- Oliver JE (1980) Monthly precipitation distribution: a comparative index. *Prof Geogr* 32(3):300–309
- Ongoma V, Chen H (2017) Temporal and spatial variability of temperature and precipitation over East Africa from 1951 to 2010. *Meteorog Atmos Phys* 129(2):131–144
- Pettitt AN (1979) A non-parametric approach to the change-point problem. *J R Stat Soc Ser C Appl Stat* 28(2):126–135
- Seleshi Y, Zanke U (2004) Recent changes in rainfall and rainy days in Ethiopia. *Int J Climatol* 24(8):973–983
- Seleshi Y, Camberlin P (2006) Recent changes in dry spell and extreme rainfall events in Ethiopia. *Theor Appl Climatol* 83(1):181–191
- Serdeczny O, Adams S, Baarsch F, Coumou D, Robinson A, Hare W, Schaeffer M, Perrette M, Reinhardt J (2017) Climate change impacts in Sub-Saharan Africa: from physical changes to their social repercussions. *Reg Environ Chang* 17(6):1585–1600
- Simane B, Zaitchik BF, Foltz JD (2016) Agro-ecosystem specific climate vulnerability analysis: application of the livelihood vulnerability index to a tropical highland region. *Mitig Adapt Strateg Glob Chang* 21:39–65
- Stojanovic M, Mulualem GM, Sorí R, Vázquez M, Nieto R, Gimeno L (2022) Precipitation Moisture Sources of Ethiopian River Basins and Their Role During Drought Conditions. *Front Earth Sci* 10:929497
- Subramanya K (2008) Engineering hydrology, in Third Edition, p 223. <https://doi.org/10.4324/9781315422770-36>
- Tekleab S, Mohamed Y, Uhlenbrook S (2013) Hydro-climatic trends in the Abay/upper Blue Nile basin, Ethiopia. *Phys Chem Earth Pt A/B/C* 61:32–42
- Tsidu GM (2012) High-resolution monthly rainfall database for Ethiopia: Homogenization, reconstruction, and gridding. *J Clim* 25(24):8422–8443
- United Nations (2019) Department of Economic and Social Affairs, Population Division (2019). In: *World Population Prospects 2019: Data Booklet (ST/ESA/SER.A/424)*. United Nations
- van der Esch S, ten Brink B, Stehfest E, Bakkenes M, Sewell A, Bouwman A, Meijer J, Westhoek H, van den Berg M, van den Born GJ, Doelman J, Berkhout E, Klein Goldewijk K, Bouwman AF, Beusen A, van Zeist W-J, Stoorvogel JJ, Schut AGT, Biemans H, ... Mantel S (2017) Exploring future changes in land use and land condition and the impacts on food, water, climate change and biodiversity: Scenarios for the UNCCD Global Land Outlook. PBL: Netherlands Environmental Assessment Agency. <http://www.pbl.nl/en/publications/exploring-future-changes-in-land-use>
- Viste E, Korecha D, Sorteberg A (2013) Recent drought and precipitation tendencies in Ethiopia. *Theor Appl Climatol* 112(3):535–551
- Wagesho N, Goel NK, Jain MK (2013) Temporal and spatial variability of annual and seasonal rainfall over Ethiopia. *Hydrol Sci J* 58(2):354–373
- Wainwright CM, Marsham JH, Keane RJ, Rowell DP, Finney DL, Black E, Allan RP (2019) ‘Eastern African Paradox’ rainfall decline due to shorter not less intense Long Rains. *npj Climate and Atmospheric Science* 2(1):1–9
- Woodfine A (2009) Using sustainable land management practices to adapt to and mitigate climate change in sub-Saharan Africa: Resource Guide Version 1.0. TerrAfrica, Washington DC, USA
- World Meteorological Organization (WMO) (2019) The Global Climate in 2015–2019. WMO, Geneva, Switzerland
- World Meteorological Organization (WMO) 2020 Press release. <https://public.wmo.int/en/media/press-release/2020-track-be-one-of-three-warmest-years-record>, accessed July 25, 2022

Publisher’s note Springer Nature remains neutral with regard to jurisdictional claims in published maps and institutional affiliations.